Mechanistic Aspects of the Alternating Copolymerization of Propene with Carbon Monoxide Catalyzed by Pd(II) Complexes of Unsymmetrical Phosphine−Phosphite Ligands

Kyoko Nozaki,*,† Naomasa Sato,† Yoichi Tonomura,† Masako Yasutomi,† Hidemasa Takaya,†,‡ Tamejiro Hiyama,† Toshiaki Matsubara,*,§ and Nobuaki Koga*,§

Contribution from the Department of Material Chemistry, Graduate School of Engineering, Kyoto University, Yoshida, Sakyo-ku, Kyoto 606-01, Japan, and School of Informatics and Sciences and Graduate School of Human Informatics, Nagoya University, Nagoya 464-01, Japan

Received September 11, 1997[⊗]

Abstract: The reaction steps responsible for the highly enantioselective asymmetric copolymerization of propene with carbon monoxide catalyzed by a cationic Pd(II) complex bearing an unsymmetrical chiral bidentate phosphine−phosphite, (*R*,*S*)-BINAPHOS [(*R*,*S*)-2-(diphenylphosphino)-1,1′-binaphthalen-2′-yl 1,1′-binaphthalene-2,2′-diyl phosphite = L^1], have been studied. Stepwise identification and characterization were carried out for catalyst precursors (*SP*-4-2)- and (*SP*-4-3)-Pd(CH_3)Cl(L^1) (**1a** and **1b**) and (*SP*-4-3)-[Pd(CH_3)(CH_3CN)(L^1)]·X^1 (X^1 = B{3,5-(CF_3)$_2C_6H_3$}$_4$) (**2**), and complexes related to the reaction steps, (*SP*-4-3)-[Pd($COCH_3$)(CH_3CN)(L^1)]·X^1 (**3**), (*SP*-4-3)- and (*SP*-4-4)-[Pd{$CH_2CH(CH_3)COCH_3$}(L^1)]·X^1 (**4a** and **4b**), (*SP*-4-3)-[Pd{$COCH_2CH(CH_3)COCH_3$}(CH_3CN)(L^1)]·X^1 (**5**), and (*SP*-4-3)-[Pd{$CH_2CH(CH_3)COCH_2CH(CH_3)COCH_3$}($L^1$)]·$X^1$ (**6**). An X-ray structure of alkyl complex **4a** has been obtained. Studies on [Pt(CH_3)$_2$(L^1)] (**8**) reveal that the methyl group is more stabilized at a position *trans* to the phosphine than at the *cis* position. This is consistent with the structures of **1**−**6** in which all carbon substituents are *trans* to the phosphine moiety in their major forms. On the basis of analogous studies using platinum complexes, an isomerization from (*SP*-4-3)-[Pd(CH_3)(CO)(L^1)]·X^1 (**13a**) to the (*SP*-4-4) isomer (**13b**) is suggested to occur for the CO-insertion process **2** → **3**, which results in the activation of the methyl group for the migration to the coordinated CO. Rapid equilibrium was observed between the two isomers **4a** and **4b** during the CO insertion process to give **5**. Theoretical studies have been carried out on the transformation of **3** to **4a** and **4b**. The B3LYP and MPn calculations indicated that the alkene insertion into the Pd−acyl bond *trans* to a phosphine is more favorable than that into the Pd−acyl bond *trans* to a phosphite. The MM3 calculations demonstrated that one specific transition structure is more favorable than the other possible transition structures for the transformation of (*SP*-4-4)-[Pd($COCH_3$)(propene)(L^1)]·X^1 (**14b**) to **4b**. The difference originates from the steric effects of the BINAPHOS ligand, and the results account for high enantio- and regioselectivities experimentally observed. The two key steps, propene insertion into **3** and CO insertion into **4**, were monitored by ^{1}H NMR spectroscopy. The activation energies for these two steps were estimated to be 19.0−19.6 kcal/mol at −20 to 0 °C, their difference being insignificant. The living nature of the copolymerization was proved. Some related chiral ligands were examined for the copolymerization. Copolymerization of other olefins with CO was also investigated.

Introduction

The alternating copolymerization of olefins with carbon monoxide is of great interest due to the potential use of the resulting polymer as a new material.[1] The process includes two of the representative reactions of a palladium complex: (1) CO insertion into an alkyl−Pd bond and (2) an olefin insertion to an acyl−Pd bond.

Insertion of CO into a transition-metal−carbon σ-bond is one of the most important steps in homogeneous catalytic processes utilizing CO, and a wide range of studies have been devoted to this subject.[2a] In contrast to the intensive studies with monodentate and C_2 symmetrical *cis* bidentate ligands,[2] less work has been reported on unsymmetrical bidentate ligand systems.[3] One of the few examples was reported by Vrieze and his co-workers in 1992. They investigated the CO insertion into a methylpalladium complex possessing a phosphorus−nitrogen ligand, 1-(dimethylamino)-8-(diphenylphosphino)naphthalene (PAN).[3b] It has been revealed that both the methyl group in Pd(CH_3)(CF_3SO_3)(PAN) and the acetyl group in Pd($COCH_3$)(CF_3SO_3)(PAN) are located *trans* to the nitrogen site. Two years later, van Leeuwen and his co-workers prepared an unsymmetrical bisphosphine ligand which consists of a diarylmonoalkenylphosphine site and a trialkylphosphine site.[3c] With Pt(II) and Pd(II) complexes of this unsymmetrical bidentate ligand, they investigated the insertion of CO into phenylplatinum and methylpalladium complexes. They reported a possible migration of the phenyl and methyl groups from *trans* to the trialkylphosphine site to *cis* and the higher activity of the former complex than the latter in migratory insertion of CO.

Compared to the CO insertion, fewer reports have appeared on the olefin insertion into an acylpalladium.[4] Direct observation of this process has been reported very recently by Rix and Brookhart using cationic 1,10-phenanthroline−Pd(II) complexes.[4f] Important reports have appeared in the last five years describing

† Kyoto University.
‡ Deceased October 4, 1995.
§ Nagoya University.
⊗ Abstract published in *Advance ACS Abstracts,* December 15, 1997.

(1) (a) Drent, E.; Budzelaar, P. H. M. *Chem. Rev.* **1996**, *96*, 663. (b) Drent, E.; van Broekhoven, J. A. M.; Budzelaar, P. H. M. *Recl. Trav. Chim. Pays-Bas* **1996**, *115*, 263. (c) Sen, A. *Acc. Chem. Res.* **1993**, *26*, 303. (d) Drent, E.; van Broekhoven, J. A. M.; Doyle, M. J. *J. Organomet. Chem.* **1991**, *417*, 235. (e) Drent, E. *Pure Appl. Chem.* **1990**, *62*, 661. (f) Sen, A. *Adv. Polym. Sci.* **1986**, *73/74*, 125. (g) Sen, A. *Chemtech* **1986**, 48.

S0002-7863(97)03199-5 CCC: $14.00

mechanistic studies on the alternating copolymerization of olefins with CO.[5] Brookhart and his co-workers have investigated the microscopic steps responsible for the alternating copolymerization of ethene with CO using the same 1,10-phenanthroline system.[5ab] On the basis of the kinetic and thermodynamic data, they proposed an accurate model for the polymer chain growth. In two other examples, stepwise isolation of the intermediates was accomplished by employing norbornene as the substrate.[5c−f] Symmetrical bidentate nitrogen ligands were used in both studies.

When α-olefins such as propene and styrene are used in place of ethene or norbornene for this copolymerization, regio- and enantioselectivities of the olefin insertion arise and the control of these becomes a problematic issue for obtaining stereoregular polyketones. In the head-to-tail copolymer, a chirotopic center exists per monomer unit. If the same enantioface of each α-olefin is selected by a catalyst, the resulting copolymer is isotactic in which all the chirotopic carbons in a polymer backbone possess the same absolute configuration. Thus, asymmetric copolymerization using chiral catalysts is now attracting much attention. Most of the successful reports on this subject deal with C_2 symmetrical bidentate ligands.[6] For example, Consiglio[6a] and Sen[6b] used Pd(II) complexes of C_2 symmetrical bisphosphines BICHEP and DUPHOS, respectively, for the asymmetric copolymerization of propene with CO. Enantioselective copolymerization of (4-*tert*-butylphenyl)-ethene with CO has been reported by Brookhart using a Pd(II)−chiral bisoxazoline complex as a catalyst.[6g] Two exceptions, phosphine−oxazoline[7a] and phosphine−phosphinite[7b] *cis* bidentate ligands, have been disclosed in very recent publications by Consiglio and by Keim, independently. Using the phosphine−oxazoline system, Consiglio improved the catalytic activity in comparison to his previous studies with bisphosphines.[7a,8] In 1995, we have demonstrated that a cationic Pd(II) complex of unsymmetrical chiral bidentate phosphine−phosphite, (*R*,*S*)-BINAPHOS [(*R*,*S*)-2-(diphenylphosphino)-1,1′-binaphthalen-2′-yl 1,1′-binaphthalene-2,2′-diyl phosphite] serves as an efficient catalyst for the asymmetric copolymerization of propene with carbon monoxide.[9] Highly isotactic polyketone was obtained in high enantioselectivity. The simplicity of the $^{13}C\{^1H\}$ NMR spectrum of the polyketone demonstrates that the tacticity control is almost complete (Chart 1). Moreover, the polymer showed the highest molar optical rotation ever reported. Our interest in the characteristic unsymmetrical feature of this bidentate ligand prompted us to explore further the mechanistic aspects of this catalyst system. In this paper we describe (1) the stepwise identification of the complexes related to the reaction steps, (2) the ligand effect of (*R*,*S*)-BINAPHOS on Pd(II) and Pt(II), (3) direct observation of the reaction process and discussion on the unseen pathways, and (4) the reaction with the related ligands and (5) with other olefins. Throughout the studies, the reaction pathway of the alternating copolymerization is demonstrated in relation to the characteristic features of the unsymmetrical bidentate ligand.

Chart 1

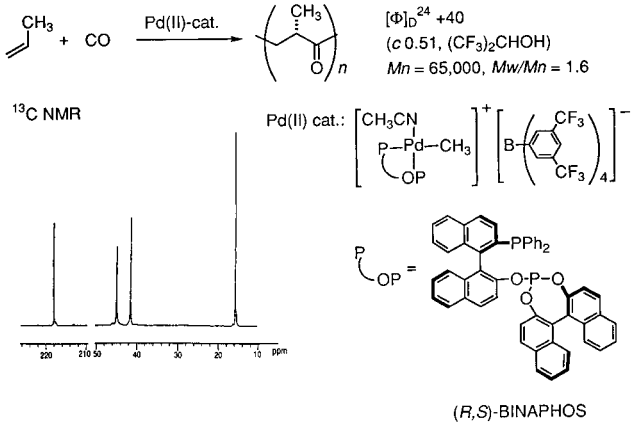

(2) For recent reviews on CO insertion with monodentate and C_2 symmetrical *cis* bidentate ligands see: (a) Colquhoun, H. M.; Thompson, D. J.; Twigg, M. V. *Carbonylation. Direct Synthesis of Carbonyl Compounds*; Plenum Press: New York, 1991. (b) Yamamoto, A.; Ozawa, F.; Osakada, K.; Huang, L.; Son, T.-I.; Kawasaki, N.; Doh, M.-K. *Pure Appl. Chem.* **1991**, *63*, 687. (c) Yamamoto, A. *J. Organomet. Chem.* **1995**, *500*, 337. For other related publications, see for example: (d) Dekker, G. P. C. M.; Elsevier, C. J.; Vrieze, K.; van Leeuwen, P. W. N. M. *Organometallics* **1992**, *11*, 1598. (e) Grushin, V. V.; Alper, H. *Organometallics* **1993**, *12*, 1890. (f) Tóth, I.; Elsevier, C. J. *J. Chem. Soc., Chem. Commun.* **1993**, 529. (g) Tóth, I.; Elsevier, C. J. *J. Am. Chem. Soc.* **1993**, *115*, 10388. (h) Kapteijn, G. M.; Dervisi, A.; Verhoef, M. J.; van den Broek, M. A. F. H.; Grove, D. M.; van Koten, G. *J. Organomet. Chem.* **1996**, *517*, 123. (i) Goren, J. H.; Elsevier, C. J.; Vrieze, K.; Smeets, W. J. J.; Spek, A. L. *Organometallics* **1996**, *15*, 3445. (j) Kayaki, Y.; Shimizu, I.; Yamamoto, A. *Bull Chem. Soc. Jpn* **1997**, *70*, 917, 1135, 1141.

(3) CO insertion with C_1 symmetrical *cis* bidentate ligands: (a) Anderson, G. K.; Lumetta, G. J. *Organometallics* **1985**, *4*, 1542. (b) Dekker, G. P. C. M.; Buijs, A.; Elsevier, C. J.; Vrieze, K.; van Leeuwen, P. W. N. M.; Smeets, W. J. J.; Spek, A. L.; Wang, Y. F.; Stam, C. H. *Organometallics* **1992**, *11*, 1937. (c) van Leewen, P. W. N. M.; Roobek, C. F.; van der Heijden, H. J. *J. Am. Chem. Soc.* **1994**, *116*, 12117. (d) Rülke, R. E.; Kaasjager, V. E.; Wehman, P.; Elsevier, C. J.; van Leeuwen, P. W. N. M.; Vrieze, K.; Fraanje, J.; Goubitz, K.; Spek, A. L. *Organometallics* **1996**, *15*, 3022. (e) Ankersmit, H. A.; Veldman, N.; Spek, A. L.; Eriksen, K.; Goubitz, K.; Vrieze, K.; van Koten, G. *Inorg. Chim. Acta* **1996**, *252*, 203. (f) Cavell, K. J.; Jin, H.; Skelton, B. W.; White, A. H. *J. Chem. Soc., Dalton Trans.* **1992**, 2923. (g) Cavell, K. J.; Jin, H.; Skelton, B. W.; White, A. H. *J. Chem. Soc., Dalton Trans.* **1993**, 1973.

(4) Olefin insertion: (a) Samsel, E. G.; Norton, J. R. *J. Am. Chem. Soc.* **1984**, *106*, 5505. (b) Brumbaugh, J.; Whittle, R. R.; Parvez, M.; Sen, A. *Organometallics* **1990**, *9*, 1735. (c) Ozawa, F.; Hayashi, T.; Koide, H.; Yamamoto, A. *J. Chem. Soc., Chem. Commun.* **1991**, 1469. (d) Markies, B. A.; Rietveld, M. H. P.; Boersma, J.; Spek, A. L.; van Koten, G. *J. Organomet. Chem.* **1992**, *424*, C12. (e) Dekker, G. P. C. M.; Elsevier, C. J.; Vrieze, K.; van Leeuwen, P. W. N. M.; Roobeek, C. F. *J. Organomet. Chem.* **1992**, *430*, 357. (f) Rix, F. C.; Brookhart, M. *J. Am. Chem. Soc.* **1995**, *117*, 1137. (g) Green, M. J.; Britovsek, G. J. P.; Cavell, K. J.; Skelton, B. W.; White, A. H. *Chem. Commun.* **1996**, 1563.

(5) Stepwise observation: (a) Brookhart, M.; Rix, F. C.; DeSimone, J. M. *J. Am. Chem. Soc.* **1992**, *114*, 5894. (b) Rix, F. C.; Brookhart, M.; White, P. S. *J. Am. Chem. Soc.* **1996**, *118*, 4746. (c) van Asselt, R.; Gielens, E. E. C. G.; Rülke, R. E.; Elsevier, C. J. *J. Chem. Soc., Chem. Commun.* **1993**, 1203. (d) van Asselt, R.; Gielens, E. E. C. G.; Rülke, R. E.; Vries, K.; Elsevier, C. J. *J. Am. Chem. Soc.* **1994**, *116*, 977. (e) Markies, B. A.; Verkerk, K. A. N.; Rietveld, M. H. P.; Boersma, J.; Kooijman, H.; Spek, A. L.; van Koten, G. *J. Chem. Soc., Chem. Commun.* **1993**, 1317. (f) Markis, B. A.; Kruis, D.; Rietveld, M. H. P.; Verkerk, K. A. V.; Boersma, J.; Kooijman, H.; Lakin, M. T.; Spek, A. L.; van Koten, G. *J. Am. Chem. Soc.* **1995**, *117*, 5263. For a theoretical study, (g) Svensson, M.; Matsubara, T.; Morokuma, K. *Organometallics* **1996**, *15*, 5568. (h) Margl, P.; Ziegler, T. *J. Am. Chem. Soc.* **1996**, *118*, 7737. (i) Margl, P.; Ziegler, T. *Organometallics* **1996**, *15*, 5519.

(6) Asymmetric synthesis: (a) Barsacchi, M.; Batistini, A.; Consiglio, G.; Suter, U. W. *Macromolecules* **1992**, *25*, 3604. (b) Jiang, Z.; Adams, S. E.; Sen, A. *Macromolecules* **1994**, *27*, 2694. (c) Bronco, S.; Consiglio, G.; Hutter, R.; Batistini, A.; Suter, U. W. *Macromolecules* **1994**, *27*, 4436. (d) Jiang, Z.; Sen, A. *J. Am. Chem. Soc.* **1995**, *117*, 4455. (e) Sperrle, M.; Consiglio, G. *J. Am. Chem. Soc.* **1995**, *117*, 12130. (f) Kacker, S.; Jiang, Z.; Sen, A. *Macromolecules* **1996**, *29*, 5852. (g) Brookhart, M.; Wagner, M. I.; Balavoine, G. G. A.; Haddou, H. A. *J. Am. Chem. Soc.* **1994**, *116*, 3641. (h) Bartolini, S.; Carfagna, C.; Musco, A. *Macromol. Rapid Commun.* **1995**, *16*, 9. (i) Bronco, S.; Consiglio, G. *Macromol. Chem. Phys.* **1996**, *197*, 355.

(7) (a) Sperrle, M.; Aeby, A.; Consiglio, G.; Pfaltz, A. *Helv. Chim. Acta* **1996**, *79*, 1387. (b) Keim, W.; Maas, H. *J. Organomet. Chem.* **1996**, *514*, 271.

(8) For papers on other improved activity with achiral catalyst systems, see for example: (a) Abu-Surrah, A. S.; Wursche, R.; Rieger, B.; Eckert, G.; Pechhold, W. *Macromolecules* **1996**, *29*, 4806. (b) Miliani, B.; Vicentini, L.; Sommazzi, A.; Garbassi, F.; Chiarparin, E.; Zangrando, E.; Mestroni, G. *J. Chem. Soc., Dalton Trans.* **1996**, 3139.

(9) Nozaki, K.; Sato, N.; Takaya, H. *J. Am. Chem. Soc.* **1995**, *117*, 9911.

Results and Discussion

1. Structure Determination of the Complexes Related to the Reaction Steps. First, we followed the reaction steps of the copolymerization by adding one monomer, either propene or CO, to the catalyst in the absence of the other monomer. In other words, alkylpalladium species were treated with carbon monoxide without propene, and acylpalladium complexes were exposed to propene in the absence of carbon monoxide. Unlike the complexes with C_2 symmetrical bidentate ligands, (*R,S*)-BINAPHOS produces *cis* and *trans* stereoisomers of square planar PdX_1X_2\{(*R,S*)-BINAPHOS\} complexes when the ligand X_1 is not equal to X_2. The structure of the observed complex for each step has been determined as follows.

1.a. Methylpalladium Chloride Complex 1. Neutral Pd(II) complex $Pd(CH_3)Cl$\{(*R,S*)-BINAPHOS\} (**1**) was used as a catalyst precursor for the present copolymerization. The compound **1** was obtained as a 5:1 mixture of two diastereomeric isomers by admixture of $Pd(CH_3)Cl(cod)$[10] and (*R,S*)-BINAPHOS. The structure of each diastereomer has been determined by ^{31}P and ^{13}C NMR spectroscopy of carbon-13-enriched **1-$^{13}CH_3$** which was prepared by disproportionation of $Pt(^{13}CH_3)_2$(cod) and $PdCl_2(PhCN)_2$ in the presence of (*R,S*)-BINAPHOS (eq 1).[11] The major isomer was assigned as **1a-$^{13}CH_3$** whose

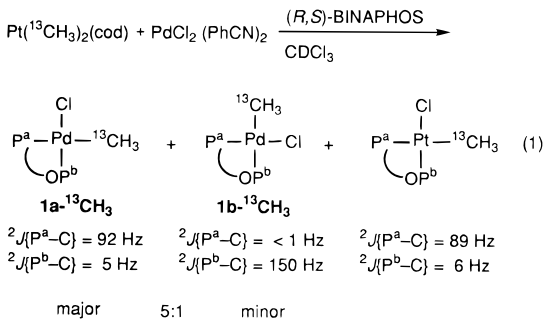

methyl group is located at a position *trans* to the phosphine site, because $^2J\{P-C\}$ in this complex was larger (92 Hz) for the methyl carbon and the phosphine than that (5 Hz) for the methyl and the phosphite.[12] The opposite order in $^2J\{P-C\}$, 150 Hz for the phosphite and less than 1 Hz for the phosphine, was observed in the minor complex, which was assigned as **1b-$^{13}CH_3$**.

The 5:1 ratio of these diastereomers seems to reflect the relative thermodynamic stability of **1a** and **1b** rather than their kinetic selectivity, which will be discussed in section 1.b. In the reaction of eq 1, a platinum complex, (*SP*-4-2)-Pt(CH_3)Cl-\{(*R,S*)-BINAPHOS\}, an analog of **1a**, was formed as a single species, simultaneously.

1.b. Cationic Methylpalladium Complex 2. A diastereomeric mixture of neutral complexes **1a-$^{13}CH_3$** and **1b-$^{13}CH_3$** was treated with $NaBAr_4$ (Ar = 3,5-$(CF_3)_2C_6H_3$) to give a cationic complex, [Pd($^{13}CH_3$)(CH_3CN)\{(*R,S*)-BINAPHOS\}]·[BAr_4] (**2-$^{13}CH_3$**), as shown in eq 2. A single species was observed by ^{31}P and ^{13}C NMR spectrometries. A large coupling constant of $^2J\{P-C\} = 78$ Hz was observed between the methyl group and the phosphine, indicating that those two were *trans* to each other.[12] The coupling between the methyl and the phosphite was less than 1 Hz.

Treatment of **2** with tetraethylammonium chloride gave an 8:1 mixture of **1a** and **1b** after 90 min and ended up in a ratio of 5:1 after 24 h at 20 °C (eq 3). This experiment suggests

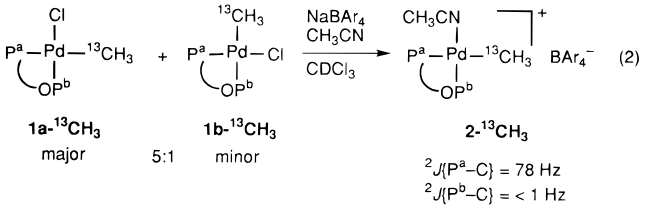

that the ratio of 5:1 for **1a** and **1b** is that controlled thermodynamically rather than kinetically (*vide supra*).

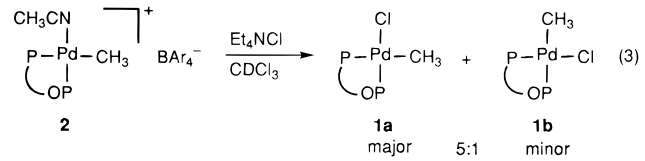

1.c. Acyl Complex 3. The structure of the acylpalladium species **3** was determined using ^{13}CO. In order to detect the methyl proton in the acetyl group by ^1H NMR, we used CD_3CN in place of CH_3CN. When a cationic complex, [Pd(CH_3)(CD_3CN)\{(*R,S*)-BINAPHOS\}]·[BAr_4] (**2-D**), was treated with 1 atm of ^{13}CO, the corresponding acyl complex, [Pd($^{13}COCH_3$)(CD_3CN)\{(*R,S*)-BINAPHOS\}]·[BAr_4] (**3-D-^{13}CO**), was obtained as a single species (eq 4). The $^2J\{C-P\}$ coupling

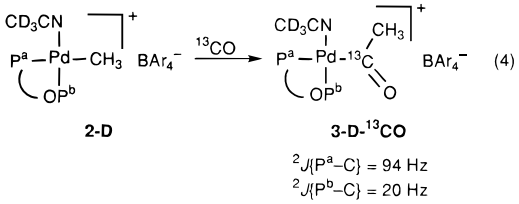

constants for the acetyl carbon were 94 Hz with the phosphine and 20 Hz with the phosphite, respectively. Those values are in good agreement with the data reported by Tóth and Elsevier for Pd($^{13}COCH_3$)(^{13}CO)\{(2*S*,4*S*)-2,4-bis(diphenylphosphino)-pentane\} in which $^2J\{C-P\}$ for the acetyl carbon was 79 Hz with its *trans* phosphorus nucleus and 19.8 Hz with its *cis* phosphorus nucleus.[2g,13] Thus, the structure of **3-D-^{13}CO** has been assigned wherein the acetyl group is placed *trans* to the phosphine. It is noteworthy that, in **3-D-^{13}CO**, acetonitrile, but not CO, coordinates to Pd under 1 atm of CO. This has been proved by the fact that the $^2J\{C-P\}$ was not observed for the coordinated CO. This is in contrast to the observation by Tóth and Elsevier in which the $^2J\{C-P\}$ was detected for the phosphorus ligand and the coordinated CO in [Pd(^{13}CO-CH_3)(^{13}CO)\{2,4-bis(diphenylphosphino)pentane\}]·[BF_4].[2g] In the present phosphine−phosphite system, the π-acidic nature of the phosphite may prefer the coordination of acetonitrile at its *trans* phosphorus nucleus because the π-acidity of acetonitrile is lower than that of CO.

1.d. Alkyl Complex 4. Olefin insertion into an acyl complex is reported to give an alkyl complex in which the ketonic oxygen coordinates to the metal to form a five-membered ring.[4,5] In

(10) Rülke, R. E.; Ernsting, J. M.; Spek, A. L.; Elsevier, C. J.; van Leeuwen, P. W. N. M.; Vrieze, K. *Inorg. Chem.* **1993**, *32*, 5769.

(11) Visser, J. P.; Jager, W. W.; Masters, C. *Recl. Trav. Chim. Pays-Bas* **1975**, *94*, 70.

(12) (a) Pidcock, A. In *Transition Metal Complexes of P-, As-, and Sb-Ligands*; McAuliffe, C. A., Ed.; Macmillan: New York, 1973; pp 1−31. (b) Hitchock, P. B.; Jacobson, B.; Pidcock, A. *J. Chem. Soc., Dalton. Trans.* **1977**, 2038 and 2043. (c) Pidcock, A.; Richards, R. E.; Venanzi, L. M. *J. Chem. Soc. A* **1966**, 1707. (d) Allen, F. H.; Pidcock, A. *J. Chem. Soc. A* **1968**, 2700.

(13) Chen reported similar $^2J\{C-P\}$ values for *cis*- and *trans*-Pd($^{13}COOCH_3$)(CH_3)(PPh_3)$_2$. The values are 163 Hz for the P−C *trans* to each other and 12 Hz for the those *cis* to each other. Chen, T. W.; Yeh, Y. S.; Yang, C. S.; Tsai, F. Y.; Huang, G. L.; Shu, B. C.; Huang, T. M.; Chen, Y. S.; Lee, G. H.; Cheng, M. C.; Wang, C. C.; Wang, Y. *Organometallics* **1994**, *13*, 4804.

this study, such alkyl complexes were obtained as a 4:1 mixture of two diastereomers. Complexes **4a** and **4b** were obtained when the acyl complex **3** was treated with propene (eq 5). At

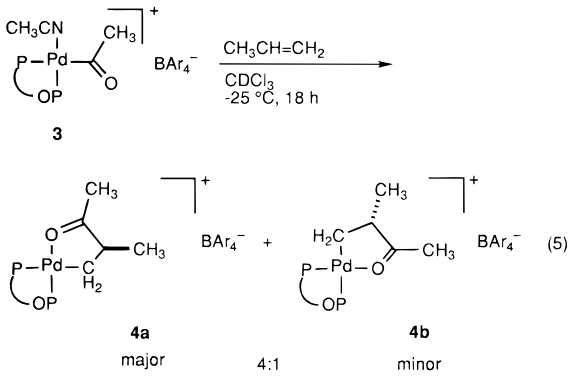

first, the structure determination of the diastereomers was carried out using carbon-13-labeled dodecene, $C_{10}H_{21}CH{=}{}^{13}CH_2$, in place of propene due to the uneasy treatment of $CH_3CH{=}{}^{13}CH_2$. Addition of $C_{10}H_{21}CH{=}{}^{13}CH_2$ to acyl complex **3** afforded two alkyl complexes, **7a** and **7b**, as a 4:1 mixture (eq 6). In the

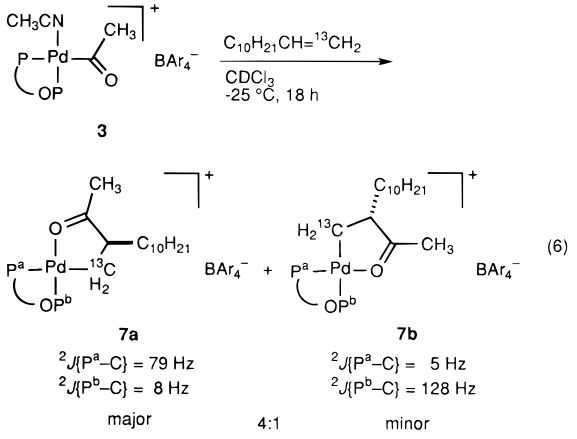

major compound, the alkyl group was determined to be *trans* to the phosphine by $^2J\{P-C\}$ in ^{31}P and ^{13}C NMR. The similarity in ^{31}P and ^{13}C NMR charts for **4** and **7** revealed that **4** is also a mixture of the diastereomers analogous to **7a** and **7b** (eq 5; see the Experimental Section for the NMR data). Rapid equilibrium seems to exist between the two diastereomers **4a** and **4b**, which will be discussed in section 3.

The 4:1 mixture of **4** was treated with CO in methanol to give the corresponding keto ester methyl (*S*)-3-methyl-4-oxopentanoate in 95% *ee* (eq 7).[9] This result is very important for

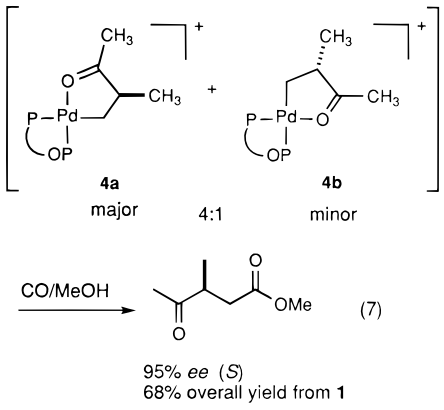

the discussion of the enantioselectivity in the alternating

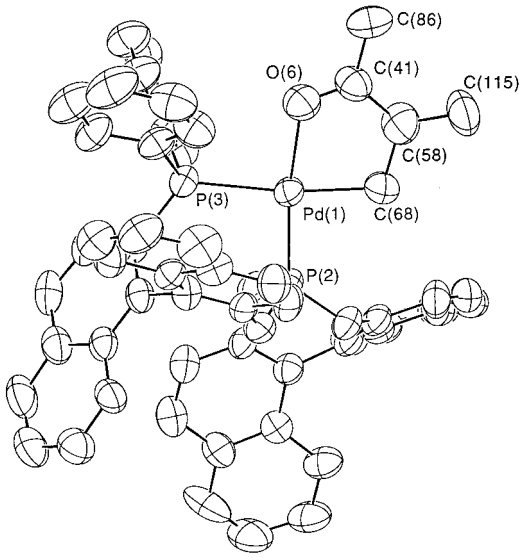

Figure 1. An ORTEP drawing for [Pd{$CH_2CH(CH_3)C(=O)CH_3$}-{(*R,S*)-BINAPHOS}]·[B{3,5-$(CF_3)_2C_6H_3$}$_4$]. The counteranion and all hydrogen atoms are omitted. Representative bond lengths (Å) and angles (deg): Pd(1)−P(2) 2.181(2), Pd(1)−P(3) 2.381(2), Pd(1)−C(68) 2.067(9), Pd(1)−O(6) 2.098(9), C(41)−O(6) 1.221(11), C(41)−C(58), 1.477(13), C(58)−C(68) 1.479(19), P(2)−Pd(1)−P(3) 96.1(1), P(2)−Pd(1)−C(68) 92.7(3), P(3)−Pd(1)−O(6) 91.8(6), O(6)−Pd(1)−C(68) 79.5(4), P(3)−Pd(1)−C(68) 171.3(3), Pd(1)−O(6)−C(41) 115.3(6), Pd(1)−C(68)−C(58) 108.9(7), O(6)−C(41)−C(82) 121.3(8), C(41)−C(58)−C(68) 111.4(9), P(2)−Pd(1)−O(6)−C(41) 5.5(11), P(2)−Pd(1)−C(68)−C(58) 160.3(7), P(3)−Pd(1)−O(6)−C(41) −170.2(7), P(3)−Pd(1)−C(68)−C(58) −19.8(14), C(68)−Pd(1)−O(6)−C(41) 9.9(7), O(6)−Pd(1)−C(68)−C(58) −19.1(7), Pd(1)−O(6)−C(41)−C(58) 2.6(7), O(6)−C(41)−C(58)−C(68) −19.6(9).

copolymerization using the present catalyst system, because it discloses that the *SSSS*... isomer is produced in more than 95% ee out of the two possible enantiomers *RRRR*... and *SSSS*.... The relation between the absolute configuration of the chirotopic carbon and the optical rotation of the polymer, that is, the *SSSS*... isomer shows positive optical rotation in $(CF_3)_2CHOH$, is consistent with the very recent studies by Bronco and Consiglio based on the sign of the CD band associated with the n → π^* transition and the application of the octant rule to the carbonyl chromophore.[6i]

The major complex **4a** was recrystallized from CH_2Cl_2 and diethyl ether and analyzed by X-ray crystallography. Its ORTEP drawing is shown in Figure 1. Two crystal structures of the five-membered alkylpalladium complexes have been reported using norbornene as the olefinic precursor.[4b,5f] Very recently, one structure of $PdCH_2CH_2COCH_3$(ligand) has been reported by Cavell and his co-workers.[4g] Accordingly, the structure of **4a** is the second example of X-ray analysis using an olefinic precursor in which β-hydride elimination is possible. The four ligands and the Pd center are almost in plane. The bite angle of the ligand P−Pd−P is 96.0°, slightly larger than the ideal angle 90° for the square planar coordination. The phosphine−Pd bond length of 2.38 Å is much longer than the phosphite−Pd bond of 2.18 Å, due to the strong *trans* influence of the alkyl group. Such a difference in the P−Pd bond length is consistent with the reported data with a bis(triphenylphosphine) complex[4b] and a bipyridine complex.[5f] In our previous communication, we assigned the coordinating oxygen in **4a** to be *trans* to the phosphine on the basis of the larger $^3J\{P-C\}$ coupling in the phosphine than in the phosphite of **4-^{13}CO** (Chart 2).[9,14] However, the above study has revealed that the $^3J\{P-$

(14) For a similar assignment, see ref 4b.

Chart 2

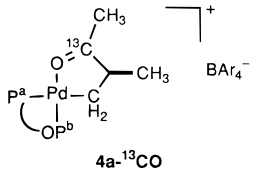

4a-^{13}CO

$^3J\{P^a-^{13}C\}$ = 10.5 Hz
$^3J\{P^b-^{13}C\}$ = 2.5 Hz

C} coupling through $^{13}C{=}O-Pd-P$ is smaller for the *trans* isomer than the *cis* isomer in this case.

1.e. Following Complexes 5 and 6. The following acyl complex **5** and alkyl complex **6** exhibited ^{31}P NMR spectra superimposable on those of the first generation acyl complex **3** and alkyl complex **4**, respectively (eq 8). Thus, **5** and **6** were

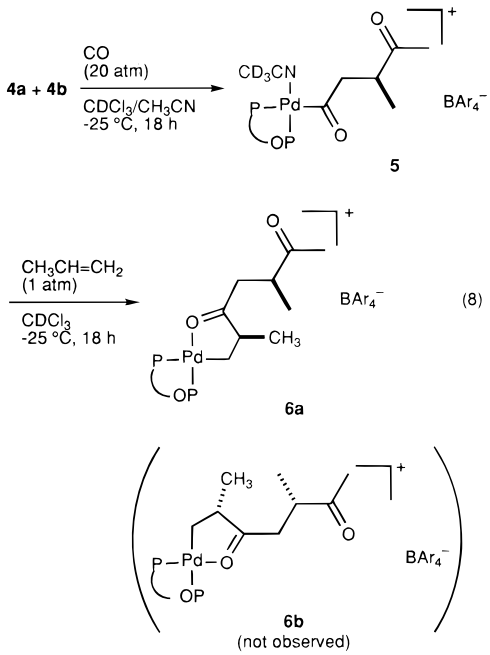

assigned to have the same *cis/trans* configuration as **3** and **4**. In the absence of acetonitrile, the δ-carbonyl in **5** weakly coordinates to the Pd center to form a six-membered ring.[5] This was observed by ^{13}C NMR as the peak broadening of the sp^2 carbon of the ketone group in the ^{13}CO-labeled **5-^{13}CO** (Figure 2a). By the addition of 1 equiv of CD_3CN, the peak was sharpened with an upfield shift, showing the formation of **5-D** (Figure 2b). The α-carbonyl, attached directly to the palladium, also upfield shifted. It is noteworthy that, among the two possible alkyl complexes **6a** and **6b**, **6a** which corresponds to **4a** was observed as a single species. The diastereomeric structure **6b** corresponding to **4b** was not detected. Due to the longer chain in **6** than in **4**, the steric bulk around the coordinating carbonyl oxygen increases in **6**. This may be the reason for the larger equilibrium constant for [**6a**]/[**6b**] than for [**4a**]/[**4b**] (the existence of the equilibrium will be discussed in section 3).

The results obtained in section 1 are summarized in Scheme 1. All the major isomers observed have either alkyl or acyl groups *trans* to the phosphine site.

2. The Stabilization and Activation Influence of (*R,S*)-BINAPHOS. In this section, we describe the higher thermodynamic stability for a methyl group *trans* to the phosphine site compared to *trans* to the phosphite site in a square planar (*R,S*)-BINAPHOS complex, $Pt(CH_3)_2$\{(*R,S*)-BINAPHOS\} (**8**).

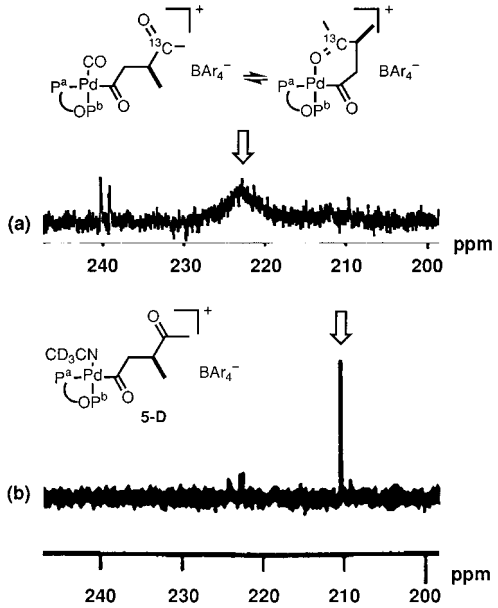

Figure 2. (a) ^{13}C NMR of $Pd[COCH_2CHCH_3COCH_3]\cdot$[(*R,S*)-BINAPHOS] in the absence of CD_3CN. The ^{13}C-labeled δ-carbonyl carbon is observed as a broad peak at δ 219−228. The α-carbonyl which is not ^{13}C-labeled is observed at δ 240 as a doublet of doublets. (b) The same in the presence of CD_3CN (**5-D**). The δ-carbonyl carbon (not labeled in this case) is sharpened at δ 210. The α-carbonyl is observed at δ 223 as a doublet of doublets.

Single-crystal X-ray analysis of **8** shows its structure in detail. As shown in Figure 3, the C−Pt distance *trans* to the phosphine is 2.102(10) Å which is possibly shorter than that *trans* to the phosphite, 2.135(12) Å $\{t = (2.135 - 2.102) \times (0.010^2 + 0.012^2)^{-1/2} = 2.1\}$. This implies that the methyl group *trans* to the phosphine site is stabilized compared to that at the *cis* position in the (*R,S*)-BINAPHOS complexes. The following NMR studies support this conclusion.

We labeled the two methyl groups of **8** with carbon-13, and compared the $^2J\{P-C\}$ to find whether each methyl group was either *cis* or *trans* to the phosphine. The representative δ and J values are summarized near formula **8-^{13}CH$_3$** in Chart 3. Generally, the coupling constant $^1J\{Pt-C\}$ is mostly consistent with the bond strength when two similar bonds are compared.[12] Here, the Pt−C bond is compared. Accordingly, the stronger Pt−C bond *trans* to the phosphine has been suggested by the larger ^1J (588 Hz) for Pt−C *trans* to the phosphine than that *trans* to the phosphite (481 Hz) (Chart 3). This tendency contradicts the generally accepted "*trans* influence order" in which phosphine is ranked at either a higher or at least even level compared to phosphite.[15]

In addition to **8-^{13}CH$_3$**, the corresponding dimethylplatinum complexes **9-^{13}CH$_3$** and **10-^{13}CH$_3$** have been prepared from (*R*)-BINAP {(*R*)-2,2′-(diphenylphosphino)-1,1′-binaphthyl} and (*R*)-BISPHOSPHITE {(*R*)-1,1′-binaphthyl-2,2′-diyl bis(diphenyl phosphite)}, respectively. When the $^1J\{Pt-C\}$ for the methyl *trans* to the phosphine is compared, the value in **8-^{13}CH$_3$** (588 Hz) is much larger than that in **9-^{13}CH$_3$** (493 Hz). At the same time, the ^1J for Pt−C *trans* to the phosphite in **8-^{13}CH$_3$** (481 Hz) is much smaller that in **10-^{13}CH$_3$** (574 Hz) (Chart 3). Rather than the *trans* relation, therefore, comparison of the *cis* relation shows better agreement, that is, between 481 Hz (**8-^{13}CH$_3$**) and 493 Hz (**9-^{13}CH$_3$**) for *cis* to the phosphines and between 588 Hz (**8-^{13}CH$_3$**) and 574 Hz (**10-^{13}CH$_3$**) for *cis* to

(15) (a) Allen, F. H.; Pidcock, A.; Waterhouse, C. R. *J. Chem. Soc. A* **1970**, 2087. (b) Appleton, T. G.; Bennett, M. A. *Inorg. Chem.* **1978**, *17*, 738.

Scheme 1

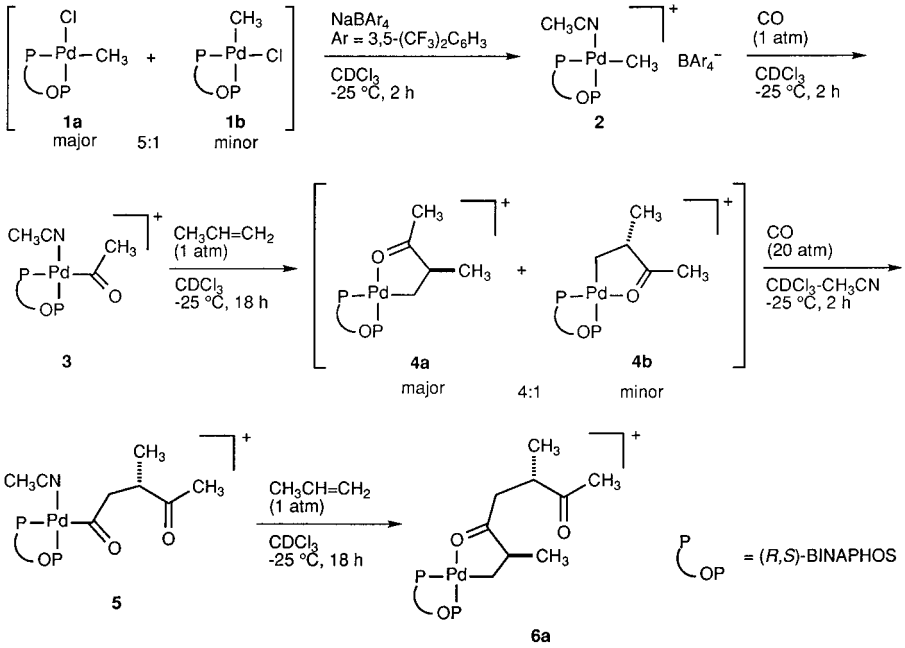

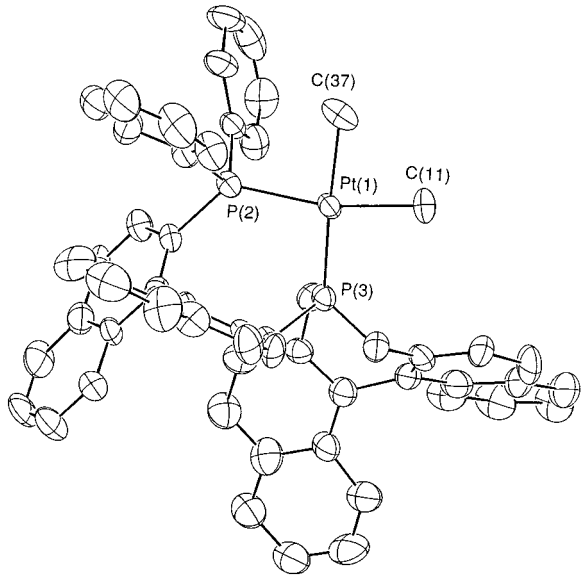

Figure 3. An ORTEP drawing for $Pt(CH_3)_2$\{(*R*,*S*)-BINAPHOS\} (**8**). All hydrogen atoms are omitted. Representative bond lengths (Å) and angles (deg): Pt(1)−C(11) 2.102(10), Pt(1)−C(37) 2.135(12), Pt(1)−P(2) 2.315(2), Pt(1)−P(3) 2.206(2), P(2)−Pt(1)−P(3) 95.2(1), P(2)−Pt(1)−C(11) 167.9(4), P(2)−Pt(1)−C(37) 86.8(4), P(3)−Pt(1)−C(11) 94.7(4), P(3)−Pt(1)−C(37) 176.4(4), C(11)−Pt(1)−C(37) 83.0(5).

the phosphites. The coupling between Pt and the protons of the methyl group (^2J\{Pt−CH_3\}) shows the same tendency.[16] Thus, apparently, the "*cis* influence" seems more significant than the *trans* influence in this system.[17] Steric factors may be another possibility for such a tendency.

Meanwhile, comparison of the ^1J\{Pt−P\} values discloses that (1) the ^1J\{Pt−P\} of the phosphine in **8** is 1602 Hz, smaller than 1874 Hz in **9**, and (2) the ^1J\{Pt−P\} of the phosphite in **8** is 3392 Hz which is larger than 3043 Hz in **10** (Chart 4). These tendencies were also observed in the corresponding $PtCl_2$(L) and $Pt(CH_3)$(Cl)(L) complexes. Thus (1) the Pt−P bond for the phosphine seems weaker in BINAPHOS complexes than in

(16) Appleton, T. G.; Clark, H. C.; Manzer, L. E. *Coord. Chem. Rev.* **1973**, *10*, 335.

(17) Allen, F. H.; Sze, S. N. *J. Chem. Soc. A* **1971**, 2054.

Chart 3

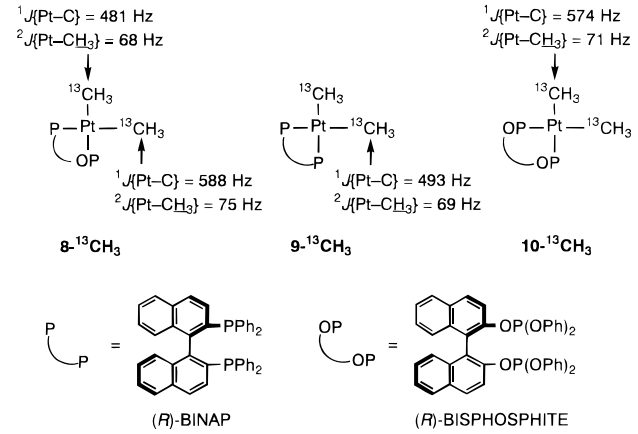

BINAP complexes, and (2) the Pt−P bond for the phosphite is stronger in BINAPHOS complexes than in BISPHOSPHITE complexes.

In summarizing this section, X-ray data combined with the NMR study have revealed that a carbon substituent, a methyl group, is stabilized *trans* to the phosphine site in (*R*,*S*)-BINAPHOS complexes. This result is consistent with the above observation in section 1 that both alkyl and acyl groups are placed *trans* to the phosphine site in all the major isomers of **1**−**6** and **7**.

3. A Proposed Pathway for the Reaction Process. In section 1, we have identified the stable complexes related to the copolymerization process. In section 3, efforts are devoted to see or predict the actual reaction pathways. The results are summarized in Scheme 2.

3.a. The First CO Insertion, 2 → 3. The insertion of CO into a carbon−metal bond in bivalent group 10 metal complexes is known to proceed through a migration. Recently, van Leeuwen and his co-workers reported an elegant example using a platinum complex of an unsymmetrical bidentate bisphosphine ligand, L−L′ = 1-(diphenylphosphino)-2-*tert*-butyl-3-(dicyclohexylphosphino)-1-propene.[3c] Migration of the phenyl group in [Pt(Ph)(solvent)(L−L′)]·[OTf] takes place in the absence of

Chart 4

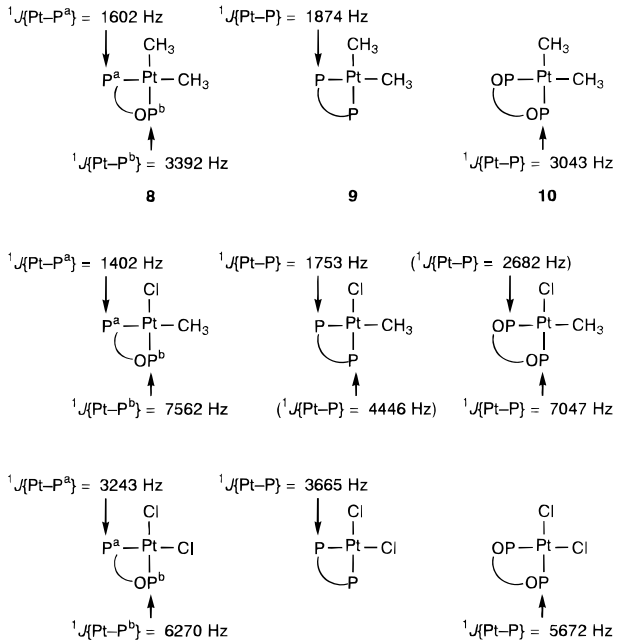

CO. Similarly, we have prepared a cationic Pt complex, [Pt(CH$_3$)(CH$_3$CN){(*R*,*S*)-BINAPHOS}]·[B{3,5-(CF$_3$)$_2$C$_6$H$_3$}$_4$] (**11**), and observed a migration of the methyl group in the presence of CO. As was so for its Pd analog **2**, the methyl group was proven to be *trans* to the phosphine by carbon-13 labeling on the methyl group. Next, the cationic Pt complex **11** was treated with CO (eq 9). At 1 atm of CO, only the replacement of CH$_3$CN to CO occurred and the carbonyl complex **12a** was observed as a single species. At elevated CO pressure (20 atm) isomerization of **12a** to **12b** took place to give a mixture of **12a**/**12b** = 1/8. Since the higher pressure was required for this isomerization, the coordination of CO to the platinum at its apical site as the fifth ligand seems to be essential for this process. After the CO pressure was released, the ratio of **12a** to **12b** was not changed. Accordingly, **12b** is the thermodynamically more stable form of **12** in which the methyl is *trans* to the phosphite. This can be attributed to the strong π-acidic nature of CO which prefers phosphine rather than phosphite at its *trans* position. In fact, the infrared absorption of the carbonyl in **12b** (ν_{CO} = 2128 cm^{-1}) suggests a slightly stronger back-donation from the platinum metal than in **12a** (2132 cm^{-1}).

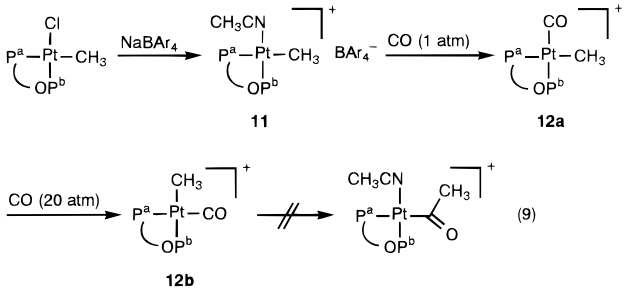

For the palladium species, van Leeuwen reported that both [Pd(CH$_3$)(solvent)(L−L′)]·(OTf) and [Pd(COCH$_3$)(solvent)(L−L′)]·[OTf] are under rapid equilibrium between their *cis/trans* isomers.[3c] In our Pd−(*R*,*S*)-BINAPHOS system, similar *cis/trans* isomerization should have also taken place either before or after the migratory CO insertion, because both the alkyl group in **2** and the acyl group in **3** are placed *trans* to the phosphine, exclusively. Although no direct evidence is obtained in the palladium system, here we presume that the methyl group in [Pd(CH$_3$)(CO){(*R*,*S*)-BINAPHOS}]·[BAr$_4$] migrates from *trans* to the phosphine to *cis* to the phosphine prior to the migration to the coordinated CO as shown in **13a** → **13b** in eq 10. This

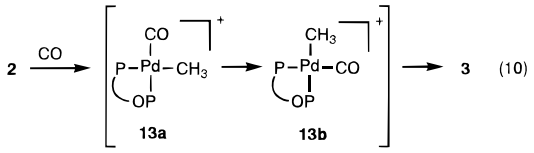

corresponds to the observation in the Pt complexes, **11** → **12a** → **12b** (eq 9). With this isomerization, the methyl group in **2** may become *more activated trans* to the phosphite than at the original position (see discussions in section 2). In this way, its migration to the coordinated CO should be accelerated to give the acyl complex **3**.[5g,18] A similar isomerization of an alkylplatinum complex prior to the migration of the alkyl group to the coordinated CO is well-known in monodentate phosphine complexes.[19]

3.b. The Subsequent CO Insertion into the Five-Membered Alkyl Complex 4. Rapid equilibrium is suggested to take place between the alkyl complexes **4a** and **4b**, on the basis of the following observations. When a 4:1 mixture of **4a** and **4b** was treated with 1 atm of CO in the presence of CH$_3$CN, the corresponding acyl complex **5** was formed as a single product. The ratio of **4a** and **4b** was determined by ^{1}H and ^{31}P NMR to be constant during the CO insertion reaction; in other words, the 4:1 ratio did not change during the CO insertion. Thus, it seems reasonable to explain this result by the rapid equilibrium between **4a** and **4b** rather than by the exactly same reactivity of **4a** and **4b** against the CO insertion. At this moment, no direct proof has yet been obtained regarding which, **4a** or **4b**, is actually involved in the catalytic process. Nevertheless, we may predict that the alkyl group could be placed *trans* to the phosphite (**4b**) prior to the CO insertion into **4** as shown in eq 11 in a manner similar to that which we proposed

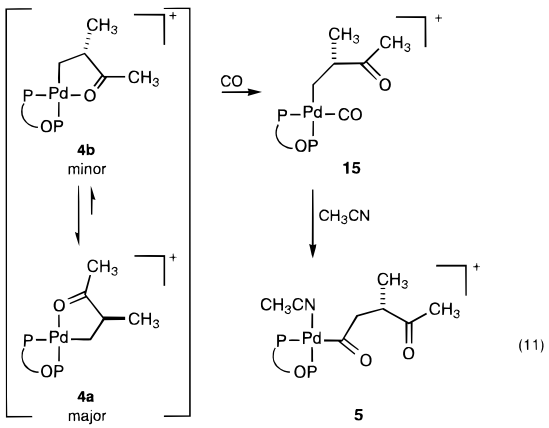

for the first CO insertion into **2** in eq 10. In this way, CO insertion proceeds from **4b** to **5** *via* **15**. For **6**, **6a** was observed as a single species and **6b** which corresponds to **4b** was not detected in the absence of CO. However, with our assumption that **4b** is more suitable for CO insertion than **4a**, the invisible **6b** might be responsible for the subsequent CO insertion.

(18) Migration of the methyl group is also suggested by theoretical studies. (a) Koga, N.; Morokuma, K. *J. Am. Chem. Soc.* **1986**, *108*, 6136. (b) Koga, N.; Morokuma, K. *Chem. Rev.* **1991**, *91*, 823.

(19) (a) Anderson, G. K.; Cross, R. J. *Acc. Chem. Res.* **1984**, *17*, 67. (b) Anderson, G. K.; Cross, R. J. *Chem. Soc. Rev.* **1980**, *9*, 185. (c) Anderson, G. K.; Clark, H. C.; Davies, J. A. *Organometallics* **1982**, *1*, 64.

Scheme 2

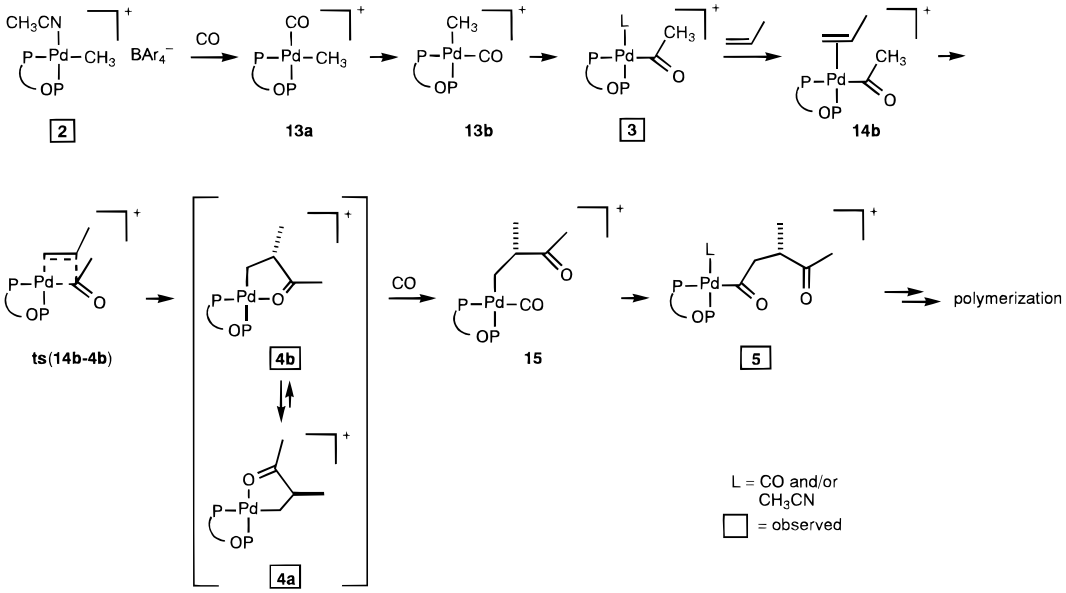

3.c. Theoretical Studies for the Olefin Insertion to Acyl Complex 3. Olefin insertion into C−M σ-bonds where M is a d^8 metal such as Ni(II), Pd(II), and Pt(II) has been of much interest not only for the olefin−CO copolymerization but also for other catalytic reactions, for example, polymerization of olefins. Intensive theoretical studies have been performed on this subject in the last decade, to show that the transition state is a four-centered metallacycle.[5g−i,20] Simply applying the theoretical results to the present experimental system, it is expected as shown in eq 12 that CH_3CN of **3** was displaced by

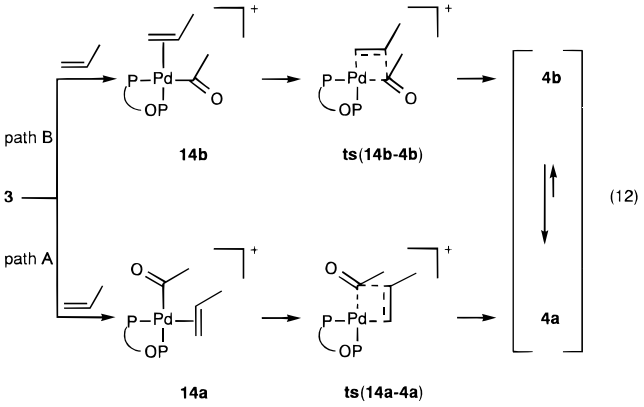

(12)

propene to give π-olefin complex **14b** or **14a** and that, passing through transition state **ts(14b-4b)** or **ts(14a-4a)**, the corresponding alkyl complexes **4b** and **4a** would be produced. In this study we have carried out theoretical calculations for the two processes **14b** → **ts(14b-4b)** → **4b** (path B) and **14a** → **ts(14a-4a)** → **4a** (path A) to investigate the mechanism of propene insertion into a Pd−acyl bond and that of enantiofacial selection.

First we investigated the mechanism of model reactions in which propene was modeled by ethene and (*R,S*)-BINAPHOS by PH_3 and $P(OH)_3$ using density functional theory and ab initio molecular orbital methods. The model reactants corresponding to **14b** and **14a** are designated as **14b′** and **14a′**, respectively, and similarly the model products as **4b′** and **4a′**. With this modeling, we could shed light on the intrinsic electronic effects of atoms or groups such as Pd, phosphine, and phosphite on the reaction. Steric effects of the bulky (*R,S*)-BINAPHOS ligand will be examined later in this section. We determined the structures of the reactants, products, and transition states (TSs) for the model reactions, as shown in Figure 4, using the density functional B3LYP method with the smaller basis set, called the B3LYP/I method. Furthermore, for the structures thus determined, the more reliable energies were calculated using the B3LYP and Møller−Plesset perturbation method with better basis set II. The energies relative to **14b′** are summarized in Table 1.[21]

Reactant **14b′** with an acyl group *trans* to the phosphine was calculated at all the levels with better basis set II to be more stable than another reactant, **14a′**, with the acyl group *trans* to the phosphite, which agrees with the experimental structure of acyl complex **3** with the acyl group *trans* to the phosphine. Product **4a′** with an alkyl ligand *trans* to the phosphine is more stable than **4b′**, also consistent with the experimental finding of the 4:1 mixture of **4a** and **4b** under thermodynamic equilibrium. The alkyl ligand as well as the acyl ligand prefers the site *trans* to phosphine, in agreement with the "stabilization influence order" experimentally found in section 2. The Pd−P bond distances in **4a′** and **4b′** show the strong *trans* influence of the alkyl ligand; the Pd−P bond *trans* to the alkyl ligand is about 0.2 Å longer, in agreement with the trend in **4a** (Figure 1).[22]

Reactions **14b′** to **4b′** and **14a′** to **4a′** pass through the tight four-centered TSs, **ts(14b′-4b′)** and **ts(14a′-4a′)**, respectively, being accompanied by the rotation of ethene from perpendicular to in-plane coordination. The calculations with basis set II show that both reactions require a comparable activation energy; the activation energies for **14b′** to **4b′** and for **14a′** to **4a′** at the B3LYP/II level are 12.8 and 12.7 kcal/mol, respectively, and those at the MP4SDQ/II level are 14.7 and 14.4 kcal/mol, respectively. Accordingly, one can conclude that the reaction from more stable and thus more populated **14b′** is more favorable than the reaction from less stable **14a′**. Product **4b′** of the more favorable reaction is less stable than **4a′**, the product

(20) Ethene insertion into a CH_3−Ni bond: (a) Musaev, D. G.; Froese, R. D. J.; Svensson, M.; Morokuma, K. *J. Am. Chem. Soc.* **1997**, *119*, 367. A carbon−carbon triple bond insertion into an acylpalladium bond: (b) Samsel, E. G.; Norton, J. R. *J. Am. Chem. Soc.* **1984**, *106*, 5505.

(21) See the Experimental Section for computational details.

(22) The calculations overestimate the Pd−P distances. It is known that the metal−P distances tend to be overestimated without phosphorous d polarization function.[23]

(23) Low, J. J.; Goddard, W. A., III; *J. Am. Chem. Soc.* **1984**, *106*, 6928.

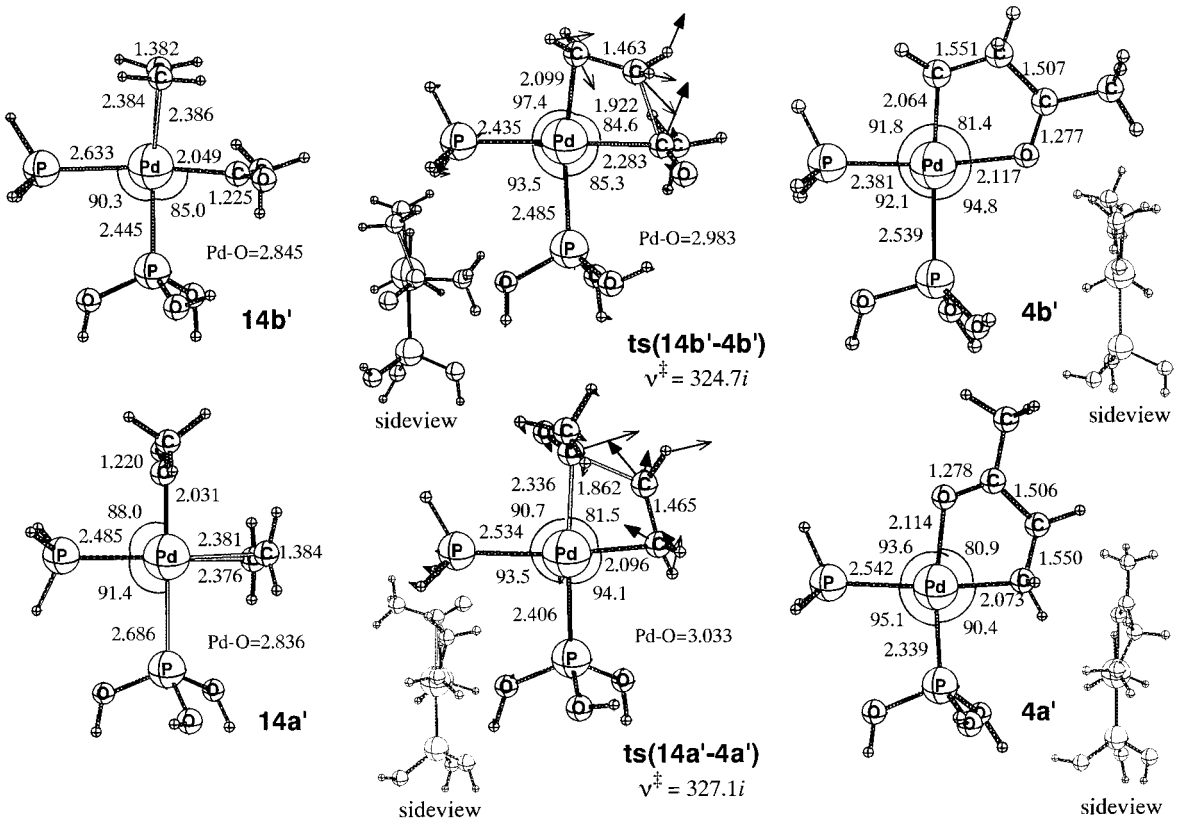

Figure 4. B3LYP/I optimized structure of model reactants **14b′** and **14a′**, transition states **ts(14b′-4b′)** and **ts(14a′-4a′)**, and products **4b′** and **4a′** in the propene insertion into the Pd−acyl bond. The phosphine and phosphite sites of (*R*,*S*)-BINAPHOS are displaced by PH_3 and $P(OH)_3$, respectively, and propene is displaced by ethene.

Table 1. Calculated Potential Energies for **14′** → **4′** Relative to **14b′** (kcal/mol) at Various Levels

	14b′	**14a′**	**ts(14b′-4b′)**	**ts(14a′-4a′)**	**4b′**	**4a′**
B3LYP/I	0.0	−0.9	11.5	16.0	−22.0	−20.9
B3LYP/II	0.0	3.5	12.8	16.2	−18.9	−21.5
MP2/II	0.0	3.5	10.3	14.5	−12.9	−16.3
MP3/II	0.0	4.0	12.9	15.5	−22.7	−25.6
MP4SDQ/II	0.0	3.5	14.7	17.9	−17.8	−20.8

Table 2. Calculated Potential Energy (ΔE), Enthalpy (ΔH), Entropy (ΔS), and Free Energy (ΔG) for **14′** → **4′** Relative to **14b′** (kcal/mol) at the B3LYP/II Level

	14b′	**14a′**	**ts(14b′-4b′)**	**ts(14a′-4a′)**	**4b′**	**4a′**
ΔE	0.0	3.5	12.8	16.2	−18.9	−21.5
ΔH^a	0.0	3.6	12.3	15.6	−17.7	−20.4
$T\Delta S^a$	0.0	1.3	−3.3	−2.4	−3.2	−3.3
ΔG^a	0.0	2.3	15.6	18.0	−14.5	−17.1

[a] ΔH, $T\Delta S$, and $\Delta G = \Delta H - T\Delta S$ calculated at 298.15 K.

of the less favorable reaction. This theoretical finding and the experimental fact that the product is a 1:4 mixture of **4b** and **4a**, which corresponds to **4b′** and **4a′**, respectively, suggest that there exists an isomerization pathway between them.

The enthalpy change calculated from the zero-point energy and thermal correction to a potential energy does not modify the trend as shown in Table 2. On the other hand, an entropy effect slightly favors **14a′** and **ts(14a′-4a′)** more than **14b′** and **ts(14b′-4b′)** to a similar extent. As a result, the free energies of activation for these paths remain to be comparable.

In the second part, the selectivity experimentally observed in propene insertion is discussed using molecular mechanics (MM) calculations in which we replaced PH_3 and $P(OH)_3$ by (*R*,*S*)-BINAPHOS and ethene by propene in the B3LYP/I optimized transition state structures. Thus, this combined MO + MM method incorporates the steric effects of the (*R*,*S*)-BINAPHOS ligand. Upon this substitution, four possible transition state structures, **I**−**IV**, are generated from each transition state. Thus, we compared their steric energies by the combined MO + MM method to show which insertion mode is the most favorable.[21] The MM3 optimized structures and relative steric energies of the four insertion modes for both paths are shown in Figure 5.

The steric energy for **Ib** was found to be the smallest among four TSs for path B. Since TS **Ib** for path B leads to **4b**, this result really accounts for the experimental result. TS **IIIb** which would result in the opposite enantioselection or **IIb** and **IVb** which would cause the opposite regioselection are less stable than **Ib** by more than 3.2 kcal/mol. As shown in Figure 5, the methyl group of propene in **IIb** and **IVb** and that in **IIIb** have closer contact with the phenyl group and the naphthalene group of the (*R*,*S*)-BINAPHOS ligand, respectively, than in **Ib**.

For path A we found that TS **Ia** which leads to **4a** is the most stable as in the case of path B. However, the other transition states, especially **IVa**, are similarly stable to **Ia**, different from the case of path B.

We also made the combined MO + MM calculations similarly for another four possible TSs of **I**−**IV** in which the enantiomers of the optimized structures by the B3LYP/I method are used and PH_3 and $P(OH)_3$ are displaced by (*R*,*S*)-BINAPHOS and ethene by propene. As shown in Figure 6, there is no explicit change in the trends of the relative steric energy of the TSs for both path A and path B. The high enantioselectivity in the propene insertion such as experimentally observed (95% ee, eq 7) will not appear if these TSs for path A are involved in the process. This also supports the above result that path B is more favorable than path A.

In summary, the B3LYP calculations and MPn calculations show that alkene insertion into the Pd−acyl bond *trans* to phosphine is more favorable than that into the Pd−acyl bond

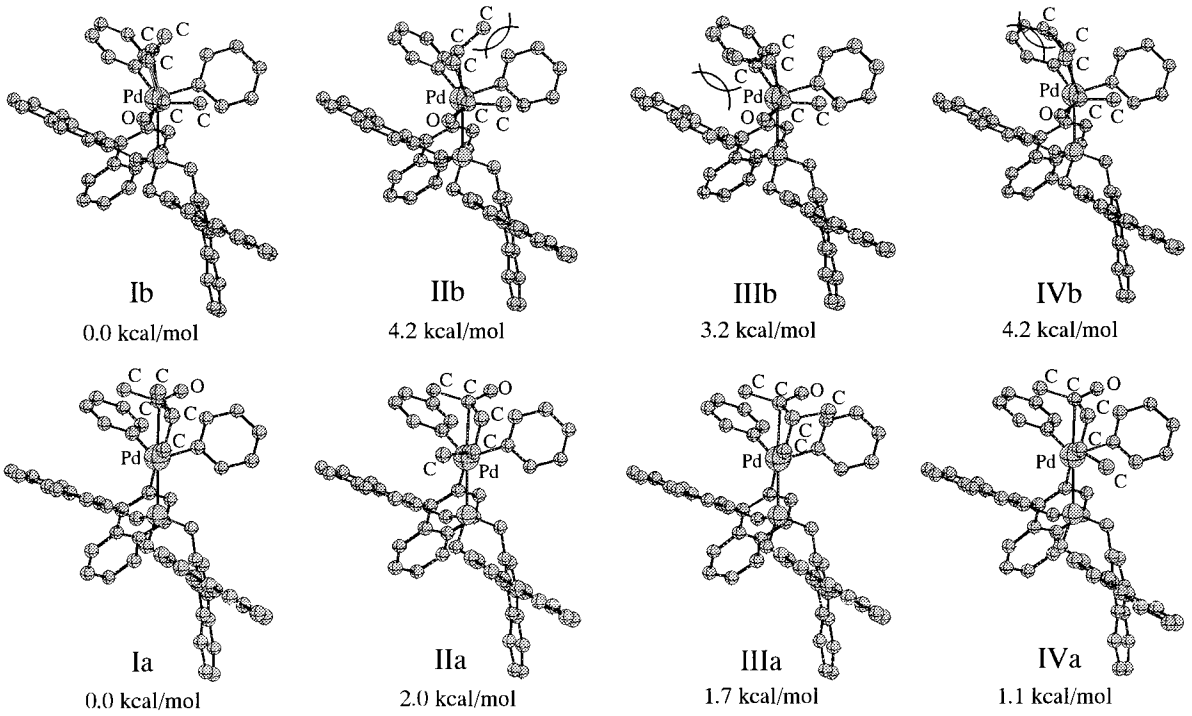

Figure 5. MM3 optimized structures and steric energies relative to **I** of the four possible isomers of TS **I**−**IV** for path B (top) and for path A (bottom) (see the text for details). All hydrogen atoms are omitted for clarity.

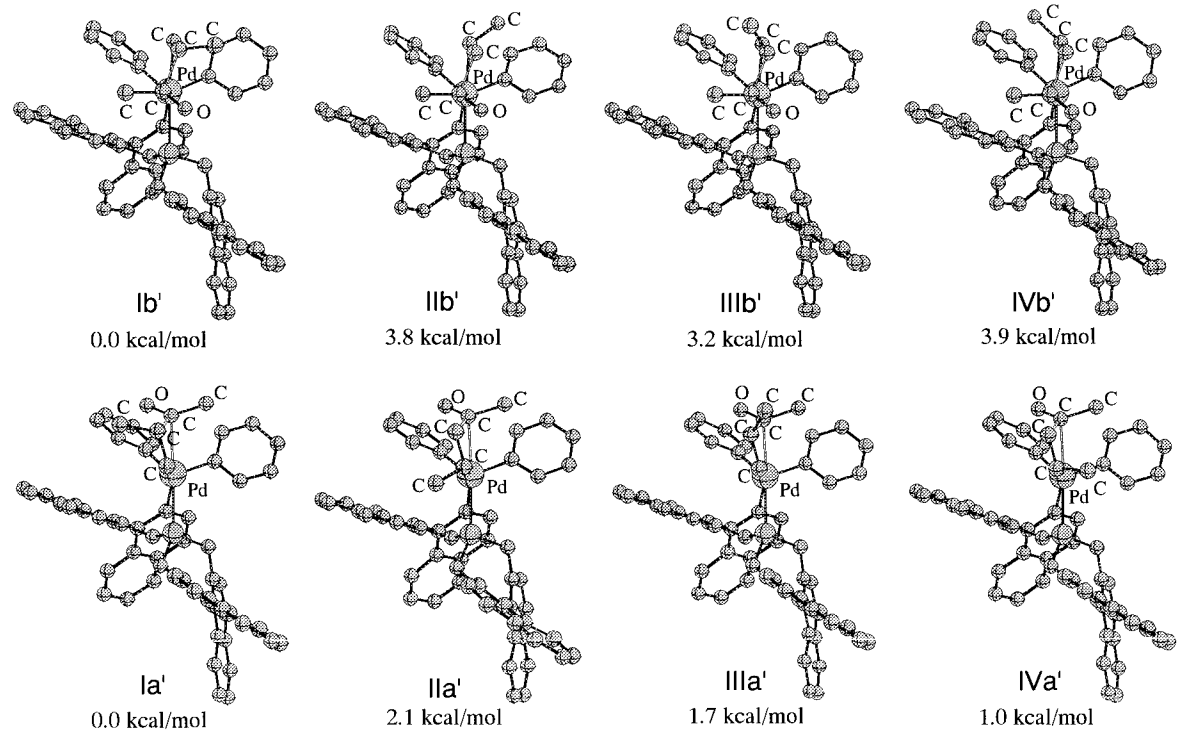

Figure 6. MM3 optimized structures and steric energies relative to **I′** of the four possible isomers of TS **I′**−**IV′** for path B (top) and for path A (bottom) (see the text for details). All hydrogen atoms are omitted for clarity.

trans to phosphite, and the MM3 calculations demonstrate that one specific transition state among four possible transition states for propene insertion with the (*R,S*)-BINAPHOS ligand is the most favorable. These results unequivocally demonstrate that the most probable path for eq 12 is **3** → **14b** → **ts(14b-4b)** → **4b** → (**4b**+**4a**).

3.d. Kinetic Studies. A kinetic study was carried out on the two representative processes of (1) propene insertion into **3** to give **4** and (2) CO insertion into **4** to give **5**. The reaction of **3** with propene was monitored by ^{1}H NMR at −10 and 0 °C. A $CDCl_3$ solution of **3** was saturated with propene (1 atm) in an NMR tube, and the conversion was monitored by ^{1}H NMR. The process was first-order in palladium complex concentration, and the observed rate constant k_{obs} was $5.3 \pm 2.0 \times 10^{-4}$ ($\Delta G^{\ddagger}$ = 19.3 ± 0.2 kcal/mol) at −10 °C as the average of five independently repeated experiments. At 0 °C, k_{obs} was 11.8×10^{-4} ($\Delta G^{\ddagger}$ = 19.6 kcal/mol). An analogous experiment with the 1,10-phenanthroline−Pd system has been reported by Brookhart and his co-workers.[5b] They determined $\Delta G^{\ddagger} = 16.6$ kcal/mol at −46 °C for the ethene insertion into Pd($COCH_3$)-(C_2H_4)(phen). The larger $\Delta G^{\ddagger}$ in our system should largely depend on the difference of the employed olefins. The reaction

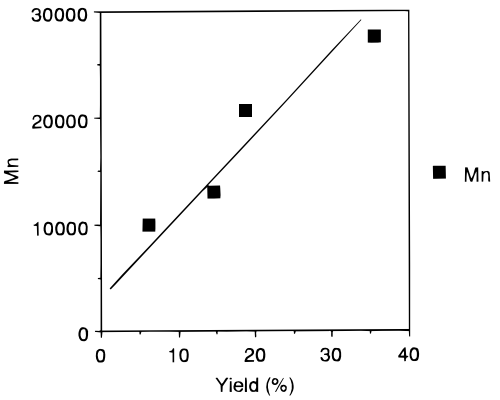

Figure 7. M_n plotted against the conversion of propene into the copolymer catalyzed by Pd(II)−(*R*,*S*)-BINAPHOS.

Chart 5

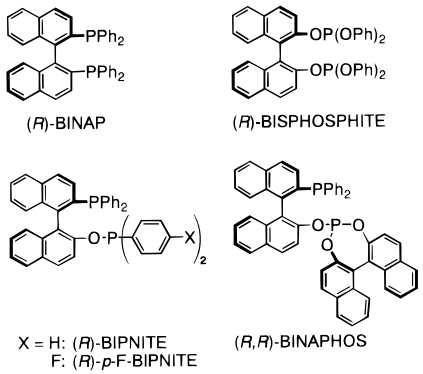

of **4** with CO was carried out in $CDCl_3$ under a CO pressure of 20 atm in an autoclave. The conversion was measured by release−repressurize of CO to measure ^{1}H NMR under 1 atm of CO at −23 °C. The process was also first-order in the concentration of the palladium complex, and k_{obs} was 1.20×10^{-4} ($\Delta G^{\ddagger} = 19.0$ kcal/mol) at −23 °C and 1.16×10^{-4} ($\Delta G^{\ddagger} = 18.9$ kcal/mol) at −12 °C. For the phenanthroline system, $\Delta G^{\ddagger} = 14.9$ kcal/mol (at −66°C) is reported for the CO insertion of $Pd(CH_2CH_2COCH_3)(CO)(phen)$.[5b] Because the two steps **2** → **4** and **4** → **5** show such close $\Delta G^{\ddagger}$, we cannot determine the rate-determining step from those results. Nevertheless, the present study provides an estimation of the activation energy ($\Delta G^{\ddagger}$) for the two steps. The characteristic feature of the present phosphine−phosphite system is the retarded CO insertion in comparison to Brookhart's 1,10-phenanthroline system.

3.e. The Chain-Terminating Step. The chain-terminating step is supposed to be the β-hydride elimination from an alkylpalladium species such as **4** and **6**.[1] The Pd−H bond formation *trans* to the phosphite may be disfavored since the σ-bond at this position has been suggested to be less stable. This may explain the highest molecular weight obtained with our catalyst although details are not clear yet. The living nature of the present copolymerization has been verified by demonstrating a linear relationship between $\langle M_n \rangle$ and the degree of monomer conversion (Figure 7). The results obtained in sections 1−3 are summarized in Scheme 2.

4. Asymmetric Copolymerization of Propene with CO Catalyzed by Pd(II) Complexes Bearing Other Ligands. In addition to (*R*,*S*)-BINAPHOS, (*R*)-BINAP, (*R*)-BISPHOSPHITE, and other related ligands illustrated in Chart 5 were examined for the asymmetric copolymerization. Neutral complexes of type $Pd(CH_3)(Cl)(ligand)$ and cationic complexes of the $[Pd(CH_3)(CH_3CN)(ligand)]\cdot[B\{3,5\text{-}(CF_3)_2C_6H_3\}_4]$ were prepared in a manner similar to that for (*R*,*S*)-BINAPHOS. Their ^{31}P NMR data are listed in Table 3. By using these cationic complexes as catalyst precursors, asymmetric copolymerization of propene with CO was examined. The catalytic activity was compared by quenching the reaction after 6 h. The yield and the molecular weight (M_n and M_w/M_n) of the resulting polyketones are also summarized in Table 3.

When a symmetrical bis(triarylphosphine), (*R*)-BINAP, was used as the ligand, both the neutral and the cationic complexes were obtained quantitatively. Nevertheless, no polymeric or oligomeric products were produced. We investigated the CO and propene insertion in a stepwise manner (eq 13). When the

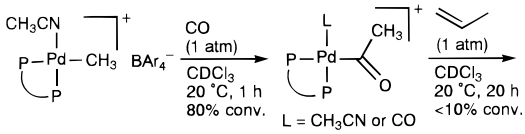

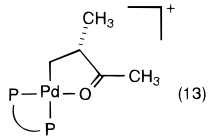

(13)

cationic complex $[Pd(CH_3)(CH_3CN)(R)\text{-BINAP}]\cdot[B\{3,5\text{-}(CF_3)_2C_6H_3\}_4]$ was treated with CO (1 atm), two acyl complexes, $[Pd(COCH_3)(L)(R)\text{-BINAP}]\cdot[B\{3,5\text{-}(CF_3)_2C_6H_3\}_4]$ in which L is either CH_3CN or CO, arose in an about 1:1 ratio. The reaction rate was comparable to that of the corresponding (*R*,*S*)-BINAPHOS complex, that is, 80% conversion with (*R*)-BINAP and 100% with (*R*,*S*)-BINAPHOS after 1 h at 20 °C. In constrast, the subsequent reaction with propene was much slower with (*R*)-BINAP than with (*R*,*S*)-BINAPHOS, that is, less than 10% conversion with (*R*)-BINAP after 20 h at 20 °C and 100% with (*R*,*S*)-BINAPHOS after 3 h at 0 °C.

On the other hand, the corresponding cationic complex was not formed when a symmetrical bis(triaryl phosphite), (*R*)-BISPHOSPHITE, was the ligand. Addition of $NaB\{3,5\text{-}(CF_3)_2C_6H_3\}_4$ to $Pd(CH_3)(Cl)\{(R)\text{-BISPHOSPHITE}\}$ at 20 °C afforded a complex mixture with which no polymerization proceeded. Recently, we reported that a phosphine−phosphinite ligand, (*R*)-BIPNITE (Chart 5), is as efficient as (*R*,*S*)-BINAPHOS in Rh(I)-catalyzed asymmetric hydroformylation of 4-vinyl-β-lactams.[24] In the present copolymerization, however, much lower activity was observed with (*R*)-BIPNITE. (*R*,*R*)-BINAPHOS, a diastereomer of (*R*,*S*)-BINAPHOS, did not form a stable cationic complex, $[Pd(CH_3)(CH_3CN)\{(R,R)\text{-BINAPHOS}\}]\cdot\{B\{3,5\text{-}(CF_3)_2C_6H_3\}_4]$. This may be attributed to the less stable coordination of the (*R*,*R*) isomer to the Pd center. In our previous study,[25] (*R*,*R*)-BINAPHOS did not form a stable apical-equatorial coordination to trigonal bipyamidal Rh(I) while (*R*,*S*)-BINAPHOS did. We explained this tendency that (*R*,*R*)-BINAPHOS requires a P−Rh−P angle much larger than 90° due to the steric repulsion of the two binaphthyl groups. This also accounts for the present result.

5. Asymmetric Copolymerization of Other Olefins with CO. Other olefins were subjected to the present copolymerization with CO.[26] (4-*tert*-Butylphenyl)ethene gave the corresponding polymer in almost complete isotacticity although both the M_n and $[\Phi]_D$ values, 5600 and −429, respectively, were lower than those reported by Brookhart[6g] (eq 14).

(24) Nozaki, K.; Wen-ge, Li.; Horiuchi, T.; Takaya, H.; Saito, T.; Yoshida, A.; Matsumura, K.; Kato, Y.; Imai, T.; Miura, T.; Kumobayashi, H. *J. Org. Chem.* **1996**, *61*, 7658.

(25) Nozaki, K.; Sakai, N.; Nanno, T.; Higashijima, T.; Mano, S.; Horiuchi, T.; Takaya, H. *J. Am. Chem. Soc.* **1997**, *119*, 4413.

(26) Kacker, S.; Jiang, Z.; Sen, A. *Macromolecules* **1996**, *29*, 5852. See also ref 6d.

Table 3. Neutral- and Cationic-Complex Formation with Other Ligands and Their Use as Catalysts for Copolymerization of Propylene and CO[a]

	^{31}P NMR				
L	$Pd(CH_3)(Cl)(L)$	$[Pd(CH_3)(CH_3CN)(L)]^+$ $[B\{3,5\text{-}(CF_3)_2C_6H_3\}_4]$	yield (%)	M_n	M_w/M_n
(*R*,*S*)-BINAPHOS	δ 149.4, 12.3 (J_{P-P} = 64.0, major) δ 154.2, 33.2 (J_{P-P} = 56.0, minor)	δ 142.9, 13.0 (J_{P-P} = 63.0)	14.6	16 400	1.07
(*R*)-BINAP	δ 39.9, 14.6 (J_{P-P} = 39.7)	δ 40.4, 14.0 (J_{P-P} = 43.5)	0	*d*	*d*
(*R*)-BISPHOSPHITE	δ 119.3, 114.7 (J_{P-P} = 91.6)	complex mixture[b]	0	*d*	*d*
(*R*)-BIPNITE	δ 136.7, 14.7 (J_{P-P} = 35.0)	δ 135.9, 16.4 (J_{P-P} = 32.8)	5.5[c]	10 200	1.40
(*R*,*R*)-BINAPHOS	δ 148.8, 18.4 (J_{P-P} = 62.6, major) and several unidentified complexes	complex mixture[b]	0	*d*	*d*

[a] The reaction was stopped after 6 h to compare the catalytic activity. [b] The cationic complex was not obtained as a single species. [c] The employed reaction time was 48 h. [d] Not determined.

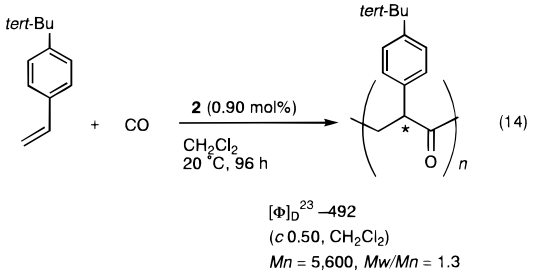

Cyclocopolymerization of α,ω-dienes with CO catalyzed by (*R*,*S*)-BINAPHOS−Pd(II) has been reported elsewhere.[27] Internal olefins such as *(E)*- and *(Z)*-2-butene were inert under the same reaction conditions. This is in sharp contrast to the report by Sen that 1,3-insertion of *(Z)*-2-butene was observed with the Me-DUPHOS−Pd(II) system.[6d] They reported that the 1,3-insertion proceeds via the Pd−H elimination−addition process shown in eq 15.

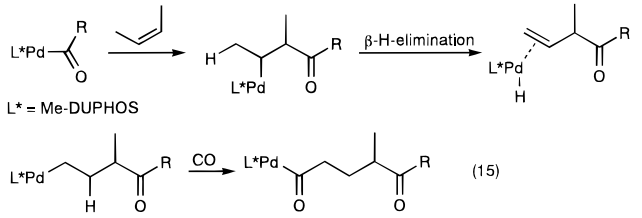

In order to clarify the sluggish step of our system, the reaction was followed stepwise. With *(E)*- and *(Z)*-2-butene, the corresponding alkylpalladium complexes were prepared by the reaction of the olefins with the acyl complex **3** (eq 16). The

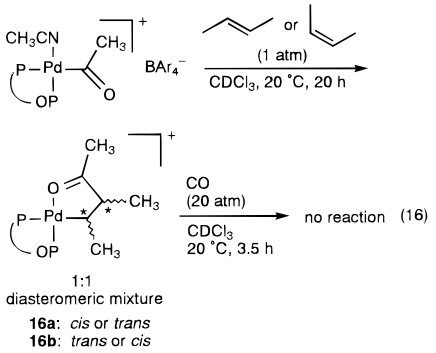

result reveals that internal olefins do insert into **3**. It is of interest that the same 1:1 diastereomeric mixture was obtained from both *(E)*- and *(Z)*-2-butene. Because both of the chemical shifts of these two diasteromers are close to that of **4a**, we tentatively assign the two diastereomers **16a** and **16b** as the *cis* and *trans* (or *trans* and *cis*) isomers of the two methyl groups on the palladacycle, respectively. When the mixture was treated with 20 atm of CO pressure for 3.5 h, no reaction was observed on the alkyl complexes **16a** and **16b**. Thus, it has been shown that the CO insertion is the key step which retarded the copolymerization of internal olefins. The methyl group on the α-carbon of the palladium center hinders the approach of CO to the metal center, and accordingly, the double-bond migration shown in eq 15 is essential for the copolymerization of 2-butene with CO to take place. In **16a** and **16b**, the absence of the Pd−H elimination−addition process may be the reason for the poor reactivity with CO. β-Elimination of the polymer chain is suggested to be the chain-termination step. The absence of β-elimination in **16a** or **16b** is consistent with the highest level of molecular weight achieved by this catalyst system.

Conclusion

The mechanism of the asymmetric copolymerization of propene with carbon monoxide catalyzed by Pd(II)−(*R*,*S*)-BINAPHOS has been disclosed as shown in Scheme 2. In the stepwise observation, all the complexes **1**−**6** have the carbon substituents *trans* to the phosphine site in their major isomers. This can be explained by the "stabilization influence" at this position in (*R*,*S*)-BINAPHOS complexes. This stabilization influence *trans* to the phosphine is characteristic for (*R*,*S*)-BINAPHOS which contradicts the conventional order of the "*trans* influence". Such an influence has been further studied in comparison with C_2 symmetrical bidentate ligands using their platinum complexes **8**−**10**. In the actual reaction condition, however, the major complexes of **1**−**6** may not be responsible for the copolymerization. We propose that the alkyl group in **2** is activated in the form of **13b** prior to its migration to the coordinated CO. Density functional and ab initio MO calculations for the model olefin insertion suggested the olefin insertion via **14b** → **ts(14b-4b)** → **4b** (path B). The calculations also gave the geometrical and energetic evidence of the above-mentioned stabilization influence, which makes another isomer of the reactant, **14a**, less stable than **14b** and thus the reaction from **14a** less favorable. The high regio- and enantioselectivities are clearly explained by the steric effect of the BINAPHOS ligand which restricts a transition structure to one specific isomeric form as shown in the combined MO + MM calculations. Some of the product **4b** isomerizes into the more stable isomer **4a** to give a 1:4 mixture of **4b** and **4a**. The equilibrium is so rapid that the 1:4 ratio does not change during the CO insertion. For the subsequent CO insertion from **4** to **5**, a speculation analogous to that for **2** to **3** is applied. In this manner, the route **4b** → **15** → **5** is suggested. For the subsequent CO insertion, **6b** rather than **6a** might be responsible.

(27) (a) Nozaki, K.; Sato, N.; Nakamoto, K.; Takaya, H. *Bull. Chem. Soc. Jpn.* **1997**, *70*, 659. (b) Borkowsky, S. L.; Waymouth, R. M. *Macromolecules* **1996**, *29*, 6377.

Related ligands such as chiral bisphosphine, bisphosphite, phosphine−phosphinite, and phosphine−phosphite were examined, but none of these showed higher activity than (*R,S*)-BINAPHOS. The copolymerization took place with 4-*tert*-butylstyrene but not with 2-butene. This suggests that the isomerization of 2-butene into a terminal olefin via β-elimination did not proceed in the alkyl complex **16**. This shows good agreement with the highest level of molecular weight achieved by this catalyst system.

Throughout the studies, we provide an example of how one unsymmetrical ligand behaves in a catalytic cycle.

Experimental Section

Preparation of Neutral Complex Pd(CH_3)(Cl){(*R,S*)-BINAPHOS} (1). A benzene (10.0 mL) solution of (*R,S*)-BINAPHOS (0.360 g, 0.468 mmol) was added to a solution of Pd(CH_3)(Cl)(COD)[10] (0.124 g, 0.468 mmol) in benzene (10.0 mL). The solution was stirred at 20 °C for 2 h, and the solution was concentrated. The crude product was reprecipitated from CH_2Cl_2 by addition of ether to give a 5:1 mixture of (*SP*-4-2)-**1** (**1a**) and (*SP*-4-3)-**1** (**1b**) (0.371 g, 86% yield). Data for **1a**: ^{1}H NMR ($CDCl_3$, 20 °C) δ 1.50 (dd, J_{P-H} = 2.6, 8.3 Hz, 3H, CH_3), 4.72 (d, J = 8.9 Hz, 1H of the ligand), 5.88 (d, J = 8.6 Hz, 1H of the ligand), 6.55−8.20 (m, 32H); ^{13}C NMR ($CDCl_3$, 20 °C) δ 9.30 (dd, J = 5, 92 Hz), 120.5−139.0 (m), 146.9−147.7 (m); ^{31}P NMR ($CDCl_3$, 20 °C) δ 12.3 (phosphine, d, J_{P-P} = 64 Hz), 149.4 (phosphite, d, J_{P-P} = 64 Hz); with partial decoupling of the aromatic protons, $^3J_{P-H}$ = 8 Hz (phosphine), ∼0 Hz (phosphite). Data for **1b**: ^{1}H NMR ($CDCl_3$, 20 °C) δ 0.51 (dd, J_{P-H} = 4.0, 11.2 Hz, CH_3), 4.68 (d, J = 11.2 Hz, 1H of the ligand), 5.84 (d, J = 9.9 Hz, 1H of the ligand), 6.55−8.20 (m, 32H); ^{31}P NMR ($CDCl_3$, 20 °C) δ 33.2 (phosphine, d, J_{P-P} = 56 Hz), 154.2 (phosphite, d, J_{P-P} = 56 Hz); with partial decoupling of aromatic protons, $^3J_{P-H}$ = ∼0 Hz (phosphine), 11 Hz (phosphite). Comparison of the $^3J_{P-H}$ values observed for CH_3 and the phosphorus atoms of (*R,S*)-BINAPHOS suggests that the methyl group is placed *trans* to the phosphine site in **1a** and *trans* to the phosphite in **1b**. Anal. Calcd for $C_{53}H_{37}ClO_3P_2Pd$: C, 68.77; H, 4.03. Found: C, 68.56; H, 3.96.

Preparation of Carbon-13-Labeled Neutral Complex Pd($^{13}CH_3$)(Cl){(*R,S*)-BINAPHOS} (1-$^{13}CH_3$). To a mixture of $PdCl_2(PhCN)_2$ (20.0 mg, 0.0520 mmol) and Pt($^{13}CH_3$)$_2$(COD) (17.6 mg, 0.0520 mmol) was added dichloromethane (2 mL), and the resulting mixture was stirred at room temperature for 15 min.[11] Addition of (*R,S*)-BINAPHOS (81.1 mg, 0.105 mmol) followed by filtration and removal of the solvent *in vacuo* afforded a 5:1 mixture of **1a**-$^{13}CH_3$ and **1b**-$^{13}CH_3$ (120.1 mg). Data for **1a**-$^{13}CH_3$: J_{C-P} = 92 Hz (phosphine), 5 Hz (phosphite). Data for **1b**-$^{13}CH_3$: J_{C-P} = ∼0 Hz (phosphine), 150 Hz (phosphite). Comparison of the $^2J_{C-P}$ values also suggests that the methyl group is placed *trans* to the phosphine site in **1a** and *trans* to the phosphite in **1b**. A platinum complex, (*SP*-4-2)-Pt($^{13}CH_3$)(Cl){(*R,S*)-BINAPHOS}, was produced simultaneously: ^{1}H NMR ($CDCl_3$, 20 °C) δ 1.30 (tdd, J_{Pt-H} = 60.0 Hz, J_{P-H} = 7.8, 3.4 Hz, CH_3), 4.66 (d, J = 8.9 Hz, 1H of the ligand), 5.86 (d, J = 8.6 Hz, 1H of the ligand), 6.55−8.20 (m, 32H); ^{13}C NMR ($CDCl_3$, 20 °C) δ 3.6 (tdd, J_{Pt-C} = 459 Hz, J_{C-P} = 89, 6 Hz), 120.5−139.0 (m), 146.9−147.7 (m); ^{31}P NMR ($CDCl_3$, 20 °C) δ 23.0 (phosphine, tdd, J_{Pt-P} = 1402 Hz, J_{P-P} = 26 Hz, J_{C-P} = 89 Hz), 115.2 (phosphite, tdd, J_{Pt-P} = 7562 Hz, J_{P-P} = 26 Hz, J_{C-P} = 6 Hz). Comparison of the $^2J_{C-P}$ values suggests that the methyl group is placed *trans* to the phosphine site in this complex.

Preparation of Cationic Complex (*SP*-4-3)-[Pd(CH_3)(CD_3CN){(*R,S*)-BINAPHOS}]·[B{3,5-(CF_3)$_2$$C_6H_3$}$_4$] (2-D). To a 5:1 mixture of **1a** and **1b** (50.8 mg, 0.0549 mmol) in CH_2Cl_2 (3.0 mL) was added a solution of NaB(3,5-(CF_3)$_2$$C_6H_3$)$_4$ (48.6 mg, 0.0549 mmol) in CD_3CN (2.0 mL). The solution was stirred at 20 °C for 2 h, and concentrated to give **2-D**: ^{1}H NMR ($CDCl_3$, 20 °C) δ 1.29 (d, J_{P-H} = 7.6 Hz, CH_3Pd), 4.74 (d, J = 8.9 Hz, 1H of the ligand), 5.98 (d, J = 8.3 Hz, 1H of the ligand), 6.66−8.27 (m, 44H); ^{13}C NMR ($CDCl_3$, 20 °C) δ 6.27 (dd, J_{P-C} = 5, 78 Hz), 117.4−135.1 (m), 139.0 (d, J = 16 Hz), 146.1, 146.7 (d, J = 28 Hz), 146.8 (d, J = 24 Hz), 161.7 (q, J = 50 Hz); ^{31}P NMR ($CDCl_3$, 20 °C) δ 13.1 (d, J_{P-P} = 64 Hz), 143.1 (d, J_{P-P} = 64 Hz).

Preparation of Carbon-13-Labeled Cationic Complex (*SP*-4-3)-[Pd($^{13}CH_3$)(CH_3CN){(*R,S*)-BINAPHOS}]·[B{3,5-(CF_3)$_2$$C_6H_3$}$_4$] (2-$^{13}CH_3$). A 5:1 mixture of **1a**-$^{13}CH_3$ and **1b**-$^{13}CH_3$ was similarly converted to the corresponding cationic complex **2**-$^{13}CH_3$ in the presence of (*SP*-4-2)-[Pt($^{13}CH_3$)(Cl){(*R,S*)-BINAPHOS}. In CH_2Cl_2−CH_3CN, the cationic Pt complex (*SP*-4-3)-[Pt($^{13}CH_3$)(CH_3CN){(*R,S*)-BINAPHOS}]·[B{3,5-(CF_3)$_2$$C_6H_3$}$_4$] (**11**-$^{13}CH_3$) gradually precipitated as a white solid while **2**-$^{13}CH_3$ remained in the solution. Filtration through a pad of Celite and removal of the solvent gave **2**-$^{13}CH_3$: J_{C-P} = 78 Hz (phosphine), ∼0 Hz (phosphite). The larger J_{C-P} value observed in the phosphine than in the phosphite disclosed that the phosphine is *trans* to the methyl group.

Addition of Chloride Anion to Cationic Complex 2. Tetraethylammonium chloride (5.0 mg, 0.0302 mmol) was added to a solution of (*SP*-4-3)-Pd(CH_3)(CD_3CN){(*R,S*)-BINAPHOS}·[B{3,5-(CF_3)$_2$$C_6H_3$}$_4$] (**2**) (0.0145 mmol) in $CDCl_3$ (0.5 mL). The reaction mixture was analyzed by NMR. After 90 min, **2** was completely converted to **1**. The ratio of **1a** and **1b** was 8:1 after 90 min, and 5:1 after 24 h.

CO Insertion To Give Acylpalladium Complex (*SP*-4-3)-[Pd(COCH$_3$)(CD_3CN){(*R,S*)-BINAPHOS}]·[B{3,5-(CF_3)$_2$$C_6H_3$}$_4$] (3-D). A solution of **2-D** in $CDCl_3$ (0.5 mL) was treated with CO (1 atm) at 20 °C to give **3-D**: ^{1}H NMR ($CDCl_3$, 20 °C) δ 2.35 (s, 3H, CH_3), 4.94 (d, J = 8.90 Hz, 1H), 6.08 (d, J = 8.58 Hz, 1H), 6.71−8.29 (m, 44H); ^{13}C NMR ($CDCl_3$, 20 °C) δ 42.1 (dd, J_{P-C} = 41, 48 Hz), 117.4−135.9 (m), 139.1 (d, J = 17 Hz), 145.6, 146.2 (d, J = 17 Hz), 146.2 (d, J = 12 Hz), 161.7 (q, J = 50 Hz), 222.4 (dd, J_{P-C} = 21, 94 Hz); ^{31}P NMR ($CDCl_3$, 20 °C) δ 10.3 (d, J_{P-P} = 113 Hz), 133.8 (d, J_{P-P} = 113 Hz); ^{19}F NMR ($CDCl_3$, 20 °C) δ −5.91; IR ($CDCl_3$) 2254, 1724 cm^{-1} (ν_{CO}). (*SP*-4-3)-[Pd(^{13}COCH$_3$)(CD_3CN){(*R,S*)-BINAPHOS}]·B{3,5-(CF_3)$_2$$C_6H_3$}$_4$ (**3-D**-^{13}**CO**) was similarly prepared from **2-D** and ^{13}CO. Data for **3-D**-^{13}**C**: J_{P-C} = 94 Hz (phosphine), 20 Hz (phosphite).

Propene Insertion To Afford Alkyl Complex [Pd($CH_2CH(CH_3)$COCH$_3$){(*R,S*)-BINAPHOS}]·B(3,5-(CF_3)$_2$$C_6H_3$)$_4$ (4). A solution of **3-D** in $CDCl_3$ (0.5 mL) was cooled to −25 °C and treated with propene (1 atm) for 14 h. The solution was concentrated at −25 °C to give a 4:1 mixture of (*SP*-4-3)-**4** (**4a**) and (*SP*-4-4)-**4** (**4b**). Data for **4a**: ^{1}H NMR ($CDCl_3$, −25 °C) δ 1.41 (d, J = 7.26 Hz, 3H, CHCH_3), 2.10 (s, 3H, C(O)CH_3), 2.34−2.45 (br, 1H, CHH), 2.75−2.89 (br, 1H, CHH), 2.98−3.15 (br, 1H, CHCH$_3$), 4.77 (d, J = 8.91 Hz, 1H), 6.02 (d, J = 8.57 Hz, 1H), 6.67−8.30 (m, 44H); ^{13}C NMR ($CDCl_3$, −25 °C) δ 20.3 (d, J_{P-C} = 4 Hz) (CH_3), 27.1 (CH_3), 39.6 (dd, J_{P-C} = 6, 79 Hz) (CH_2), 55.8 (d, J_{P-C} = 5 Hz) (CH), 117.4−134.9 (m), 139.1 (d, J = 18 Hz), 146.1, 146.6 (d, J = 11 Hz), 161.7 (q, J = 50 Hz), 240.3 (dd, J_{P-C} = 2, 10 Hz); ^{31}P NMR ($CDCl_3$, −25 °C) δ 13.0 (d, J_{P-P} = 66 Hz), 142.4 (d, J_{P-P} = 66 Hz). Data for **4b**: ^{31}P NMR ($CDCl_3$, −25 °C) δ 30.3 (d, J_{P-P} = 66 Hz), 150.3 (d, J_{P-P} = 66 Hz). Data for the mixture: ^{19}F NMR ($CDCl_3$, −25 °C) δ −5.99; IR ($CDCl_3$) 1710 (CO) cm^{-1}. The carbon-13-labeled [Pd((*R,S*)-BINAPHOS)($CH_2CH(CH_3)$^{13}COCH$_3$)]·[B(3,5-(CF_3)$_2$$C_6H_3$)$_4$] (**4**-^{13}**CO**) was similarly prepared from ^{13}CO to give a 4:1 mixture of **4a**-^{13}**CO** and **4b**-^{13}**CO**. Data for **4a**-^{13}**CO**: ^{1}H NMR ($CDCl_3$, −25 °C) δ 1.35−1.50 (m, 3H, CHCH_3), 2.10 (d, J = 5.61 Hz, 3H, C(O)CH_3), 2.34−2.45 (br, 1H, CHH), 2.75−2.89 (br, 1H, CHH), 2.98−3.15 (br, 1H, CHCH$_3$), 4.77 (d, J = 8.91 Hz, 1H), 6.02 (d, J = 8.57 Hz, 1H), 6.67−8.30 (m, 44H); ^{13}C NMR ($CDCl_3$, −25 °C) δ 117.4−134.9 (m), 139.1 (d, J = 18 Hz), 146.1, 146.6 (d, J = 11 Hz), 161.7 (q, J = 50 Hz), 240.2 (dd, J_{P-C} = 2, 10 Hz); ^{31}P NMR ($CDCl_3$, −25 °C) δ 13.0 (dd, J_{P-C} = 10, J_{P-P} = 66 Hz), 142.4 (d, J_{P-P} = 66 Hz); ^{19}F NMR ($CDCl_3$, −25 °C) δ −5.99. Data for **4b**-^{13}**CO:** ^{31}P NMR ($CDCl_3$, −25 °C) δ 30.3 (d, J_{P-P} = 66 Hz), 150.3 (dd, J_{P-C} = 11 J_{P-P} = 66 Hz).

Preparation of 1-Dodecene-1-^{13}*C*. First, $^{13}CH_3PPh_3I$ was prepared. To the solution of triphenylphosphine (1.68 g, 6.41 mmol) in toluene (20 mL) was added iodomethane-^{13}*C* (0.400 mL, 6.38 mmol). White precipitate formed, and the suspension was stirred at room temperature for 3 h. The white precipitates were collected by filtration, washed with hexane, and dried to give 1-dodecene-1-^{13}*C* in 51% yield (1.31 g): ^{1}H NMR ($CDCl_3$) δ 3.25 (dd, J_{C-H} = 135 Hz, J_{P-H} = 13.2 Hz, 3H), 7.6−7.9 (m, 15H). ^{31}P NMR ($CDCl_3$) δ 22.4 (d, J_{C-P} = 58 Hz). To a suspension of $^{13}CH_3PPh_3I$ (1.29 g, 3.18 mmol) in diethyl ether (10 mL) was added potassium *tert*-butoxide (425.6 mg, 3.79 mmol) at 0 °C. The suspension turned yellow and was stirred for 10 min. Undecanal (0.7 mL, 3.39 mmol) was added, and the whole was stirred

at room temperature for 20 h. Water was added to the reaction mixture, and the aqueous layer was extracted with diethyl ether. The combined organic layer was dried with magnesium sulfate and concentrated under reduced pressure. The crude product was purified by silica-gel column chromatography (hexane) and distilled under reduced pressure to give a colorless liquid (427.0 mg, 79%): ^{13}C NMR ($CDCl_3$) δ 114.1.

Preparation of Alkylpalladium Complex 7 from 1-Dodecene-1-^{13}C. Neutral complex **1** (19.3 mg, 0.0208 mmol) and Na[B(C_6H_3-3,5-$(CF_3)_2$)$_4$] (19.2 mg, 0.0217 mmol) were mixed in dichloromethane (2 mL) and acetonitrile (0.2 mL) at room temperature for 1 h. After removal of the solvent, the residue was dissolved in dichloromethane (2 mL), and to this was introduced carbon monoxide (1 atm). After 2 h, 1-dodecene-1-^{13}C (50 μL, 0.22 mmol) was added to the reaction mixture and stirred at room temperature for 2 h. The resulting solution was then concentrated and dried *in vacuo* to give a 4:1 mixture of **7a** and **7b** as a red solid. Data for **7a**: ^{31}P NMR ($CDCl_3$) δ 13.7 (dd, J_{C-P} = 80 Hz, J_{P-P} = 67 Hz), 141.1 (dd, J_{C-P} = 8 Hz, J_{P-P} = 67 Hz); ^{13}C NMR ($CDCl_3$) δ 37.0 (dd, J_{P-C} = 80, 8 Hz). Data for **7b**: ^{31}P NMR ($CDCl_3$) δ 29.5 (dd, J_{C-P} = 5 Hz, J_{P-P} = 64 Hz), 150.0 (dd, J_{C-P} = 128 Hz, J_{P-P} = 66 Hz); ^{13}C NMR ($CDCl_3$) δ 46.8 (dd, J_{P-C} = 128, 5 Hz). Comparison of J_{C-P} values disclosed the structures of **7a** and **7b**.

Carbomethoxylation of the Alkylpalladium Complex 4. To a 5:1 mixture of **1a** and **1b** (81.2 mg, 0.0877 mmol) in CH_2Cl_2 (2.5 mL) was added a solution of NaB(3,5-$(CF_3)_2C_6H_3)_4$ (77.7 mg, 0.0877 mmol) in CH_3CN (0.5 mL). The solution was stirred at 20 °C for 1 h, and the solution was concentrated. The resulting crude **2** was then dissolved with $CHCl_3$, and the solution was degassed by three cycles of freeze−thaw. After the solution was treated with CO (1 atm) for 0.5 h, the solution was cooled to −25 °C and treated with propene (1 atm) for 21 h. The solvents were evaporated at −25 °C to give **4** *in situ*. A solution of this crude **4** in $CHCl_3$ (2.0 mL) and CH_3OH (1.0 mL) was treated with CO (20 atm) at −25 °C for 4 days. After release of CO pressure, the solvent was evaporated and the residue was purified by distillation (80 °C, 1.0 Torr) to give methyl (*S*)-2-methyl-4-oxopentanoate in 68% total yield from **1**. The enantiomeric excess of the product (95% ee) was determined by GLC with a chiral column (Chrompack CP-cyclodextrin-β-236M-19, 100 °C). Data for methyl (*S*)-2-methyl-4-oxopentanoate: ^{1}H NMR ($CDCl_3$) δ 1.43 (d, J = 7.26 Hz, 3H, CHCH_3), 2.22 (s, 3H, C(O)CH_3), 2.30 (dd, J = 16.83, 5.61 Hz, 1H, CHH), 2.77 (dd, J = 16.83, 8.58 Hz, 1H, CHH), 2.95−3.06 (m, 1H, CHCH$_3$), 3.66 (s, 3H, COOCH_3). The absolute configuration was determined to be *S* by comparison of the optical rotation value with the literature data.[28] $[\alpha]^{25}_D$ = −54° (*c* 0.42, THF).

Crystal Data for 4a. A single crystal of **4a** ($C_{89}H_{65}BF_{24}O_4P_2Pd$, M = 1833.70) was obtained from hexane/dichloromethane solution. Data were collected on a Mac Science MXC18 diffractometer (Cu Kα, λ = 1.541 78 Å), $2\theta_{max}$ = 60°. Three standard reflections were measured every 100 reflections at 220 K. Of the 9248 reflections which were collected, 8068 were unique (R_{int} = 0.031). The crystal structure was solved by direct methods (SIR92). The non-hydrogen atoms were refined anisotropically. Hydrogen atoms were placed in fixed calculated positions. The final cycle of full-matrix least-squares refinement was based on 6986 observed reflections ($I > 3.00\sigma$) and 1144 variable parameters and converged with unweighted and weighted agreement factors of $R = \sum||F_o| - |F_c||/\sum|F_o| = 0.0901$ and $R_w = (\sum w(|F_o| - |F_c|)^2/\sum wF_o^2)^{0.5} = 0.0964$. Orthorhombic, space group $P2_12_12_1$, a = 20.9034(4) Å, b = 29.9506(7) Å, c = 12.7725(9) Å, V = 7796.45(6) Å^3, d_{calcd} = 1.50 g/cm^3, Z = 4. Details are given in the Supporting Information.

CO Insertion To Give the Second-Generation Acylpalladium Complex (*SP*-4-3)-[Pd(COCH$_2$CH(CH$_3$)COCH$_3$)(CD$_3$CN){(*R*,*S*)-BINAPHOS}]·[B{3,5-(CF$_3$)$_2$C$_6$H$_3$}$_4$] (5-D). A 4:1 mixture of **4a** and **4b** in $CDCl_3$ (0.5 mL) and CD_3CN (0.03 mL) was treated with CO (20 atm) at −25 °C to give **5-D**: ^{1}H NMR ($CDCl_3$, −25 °C) δ 1.19 (d, J = 6.93 Hz, 3H, CHCH_3), 2.12 (s, 3H, COCH_3), 2.94 (br d, J = 17.81 Hz, 1H), 3.19−3.38 (m, 1H), 3.41−3.64 (m, 1H), 4.58 (d, J = 9.24 Hz, 1H), 5.87 (d, J = 8.57 Hz, 1H), 6.58−8.21 (m, 44H); ^{13}C NMR ($CDCl_3$, −25 °C) δ 16.3, 28.5, 42.8, 56.6 (dd, J_{P-C} = 36, 74 Hz), 117.0−135.1 (m), 138.7 (d, J = 17 Hz), 145.7−146.5 (m), 161.5 (q, J = 50 Hz), 210.3, 223.3 (dd, J_{P-C} = 21, 100 Hz); ^{31}P NMR ($CDCl_3$, −25 °C) δ 9.7 (d, J_{P-P} = 108 Hz), 137.0 (d, J_{P-P} = 108 Hz); ^{19}F NMR ($CDCl_3$, −25 °C) δ −5.71; IR ($CDCl_3$) 1716, 1612 (ν_{CO}) cm^{-1}.

Propene Insertion To Give the Second-Generation Alkylpalladium Complex [Pd(CH$_2$CH(CH$_3$)COCH$_2$CH(CH$_3$)COCH$_3$){(*R*,*S*)-BINAPHOS}]·[B{3,5-(CF$_3$)$_2$C$_6$H$_3$}$_4$] (6). A solution of **5-D** in $CDCl_3$ (0.5 mL) and CD_3CN (0.03 mL) was treated with propene (1 atm) at −25 °C for 48 h. The solution was concentrated at −25 °C to give (*SP*-4-3)-**6** (**6a**) as a single product. Data for **6a**: ^{1}H NMR ($CDCl_3$, −25 °C) δ 0.85 (d, J = 7.26 Hz, 3H, CHCH_3COCH$_3$), 1.39 (s, 3H, C(O)CH_3), 1.58 (d, J = 7.26 Hz, 3H, CHCH_3COCH$_2$), 2.07−2.32 (m, 2H, CHCH$_3$COCH$_3$ and COCHH), 2.35−2.50 (m, 1H, PdCHH), 2.69−2.80 (m, 1H, PdCHH), 3.06−3.30 (m, 2H, COCHH and CHCH$_3$-COCH$_2$), 4.65 (d, J = 8.90 Hz, 1H), 5.99 (d, J = 8.58 Hz, 1H), 6.68−8.29 (m, 44H); ^{13}C NMR ($CDCl_3$, −25 °C) δ 15.9, 21.5, 27.1, 40.5 (dd, J_{P-C} = 7, 93 Hz), 41.3, 41.3, 55.4 (d, J_{P-C} = 6 Hz), 117.0−136.2 (m), 138.7 (d, J = 16 Hz), 146.0, 146.3 (d, J = 11 Hz), 161.5 (q, J = 50 Hz), 209.0, 240.4 (dd, J_{P-C} = 4, 9 Hz); ^{31}P NMR ($CDCl_3$, −25 °C) δ 13.1 (d, J_{P-P} = 67 Hz), 142.0 (d, J_{P-P} = 67 Hz); ^{19}F NMR ($CDCl_3$, −25 °C) δ −5.74; IR ($CDCl_3$) 1712, 1641 (ν_{CO}) cm^{-1}.

Preparation of Pt($^{13}CH_3$)$_2$(COD). At first, $^{13}CH_3MgI$ was prepared. To a mixture of magnesium turnings (103.3 mg, 4.25 mmol) in ether (5 mL) was added dropwise $^{13}CH_3I$ in ether (0.70 M solution, 5 mL, 3.5 mmol). The solution turned brown. After the solution was stirred for 2 h, the supernatant was transferred to a Schlenk tube and stored under argon. The corresponding Grignard reagent $^{13}CH_3MgI$ (0.17 M) was obtained. To a yellow suspension of PtI_2(COD) (147.5 mg, 0.26 mmol) in ether (5 mL) was added $^{13}CH_3MgI$ in ether (0.17 M, 3 mL, 0.51 mmol) dropwise at 0 °C. The suspension turned to a clear solution. After being stirred at 0 °C for 1.5 h, the solution was quenched with saturated NH_4Cl(aq) and then extracted with ether (3 × 10 mL). The ether layer was collected and evaporated under reduced pressure. The crude product was purified by silica-gel colunm chromatography (CH_2Cl_2/hexane = 1/2) to give a white solid (125.5 mg, >99% yield): ^{1}H NMR ($CDCl_3$) δ 0.74 (J_{Pt-H} = 82.2 Hz, J_{C-H} = 128, 1.7 Hz), 2.2−2.4 (m), 4.7−4.9 (m).

Preparation of Pt(CH$_3$)$_2${(*R*,*S*)-BINAPHOS} (8 and 8-$^{13}CH_3$). To a mixture of Pt(CH_3)$_2$(COD) (52.2 mg, 0.16 mmol) and (*R*,*S*)-BINAPHOS (119.8 mg, 0.16 mmol) was added dichloromethane (5 mL), and the solution was stirred at room temperature for 1.5 h. The reaction mixture was concentrated and dried *in vacuo*. Purification by silica-gel column chromatography (CH_2Cl_2/hexane = 1/1) gave the product (89.3 mg, 57% yield). The carbon-13-labeled **8-$^{13}CH_3$** was similarly prepared from Pt($^{13}CH_3$)$_2$(COD). Data for **8**: ^{1}H NMR ($CDCl_3$) δ 0.00 (J_{Pt-H} = 68.3 Hz, CH_3 *trans* to phosphite), 1.00 (J_{Pt-H} = 74.9 Hz, CH_3 *trans* to phosphine), 4.70 (d, J = 8.9 Hz, 1H of aromatic), 5.88 (d, J = 8.3 Hz, 1H of aromatic), 6.5−8.2 (m, aromatic); ^{31}P NMR ($CDCl_3$) δ 21.4 (J_{Pt-P} = 1602 Hz, J_{P-P} = 18 Hz, phosphine), 159.0 (J_{Pt-P} = 3392 Hz, J_{P-P} = 18 Hz, phosphite). Anal. Calcd for $C_{54}H_{40}O_3P_2Pt$: C, 65.25; H, 4.06. Found: C, 65.14; H, 3.85. From **8-$^{13}CH_3$**, the following data were given: ^{31}P NMR J_{C-P} = 90, 8 Hz (phosphine), 155, 9 Hz (phosphite); ^{13}C NMR ($CDCl_3$) δ 0.1 (J_{Pt-C} = 588 Hz, J_{P-C} = 90 Hz, J_{C-C} = 8.6 Hz, *trans* to phosphine), 6.7 (J_{Pt-C} = 481 Hz, J_{P-C} = 155 Hz, J_{C-C} = 8.6 Hz, *trans* to phosphite). Assignment of the carbon and proton peaks to carbons and protons either *cis* or *trans* to the phosphine or the phosphite was carried out by the following procedure. For the phosphorus nucleus at δ 21.4 (phosphine) by ^{31}P NMR, the larger J_{C-P} (90 Hz) should arise from the coupling with the carbon at its *trans* nucleus. This J_{C-P} value is seen in the ^{13}C NMR peak at δ 0.1. Similarly, J_{C-P} of 155 Hz is common for the phosphite peak at δ 159.0 (^{31}P NMR) and the ^{13}C NMR peak at δ 6.7. Measurement of ^{13}C NMR with decoupling of individual proton peaks revealed that the proton at δ 0.00 (^{1}H NMR) is attached to the carbon at δ 6.7 (^{13}C NMR) and that the proton at δ 1.00 (^{1}H NMR) is attached to the carbon at δ 0.1 (^{13}C NMR).

Crystal Data for 8. A single crystal of **8** ($C_{54}H_{40}O_3P_2Pt$, M = 993.94) was obtained from hexane/ethyl acetate solution. Data were collected on a Mac Science MXC18 diffractometer (Cu Kα, λ = 1.541 78 Å), $2\theta_{max}$ = 60°. Three standard reflections were measured every 100 reflections at 297 K. The unique 5167 reflections with $I > 3\sigma(I)$ were considered as observed. The crystal structure was solved

(28) (a) Blanco, L.; Rousseau, G.; Barnier, J.-P.; Guibé-Jampel, E. *Tetrahedron: Asymmetry* **1993**, *4*, 783. (b) Enders, D.; Gerdes, P.; Kipphardt, H. *Angew. Chem., Int. Ed. Engl.* **1990**, *29*, 179.

by the direct method (SIR 92). The non-hydrogen atoms were refined anisotropically. Hydrogen atoms were placed in fixed calculated positions. A series of standard full-matrix least-squares refinement and Fourier synthesis revealed the remaining atoms. All calculations were performed using the Crystan crystallographic software package. Current residual values for 603 parameters are $R = 0.0594$ and $R_w = 0.0712$. Orthorhombic, space group $P212121$, FW = 993.94 $a = 17.2570$ (25) Å, $b = 28.9158$ (45) Å, $c = 9.9413$ (22) Å, $V = 4960.68$ (152) Å^3, $d_{calcd} = 1.663$ g/cm^3, $Z = 5$. Details are given in the Supporting Information.

Preparation of Pt(CH$_3$)$_2$\{(*R*)-BINAP\} (9 and 9-^{13}CH$_3$). To a mixture of Pt(CH$_3$)$_2$(COD) (25.6 mg, 0.077 mmol) and (*R*)-BINAP (49.3 mg, 0.077 mmol) was added chloroform (5 mL), and the solution was stirred at 40 °C for 20 h. The reaction mixture was concentrated and dried *in vacuo.* Purification by silica-gel column chromatography (CH_2Cl_2/hexane = 1/2) gave the product (47.9 mg, 73% yield): ^{1}H NMR ($CDCl_3$) δ 0.34 (J_{Pt-H} = 69.3 Hz), 6.6−7.7 (m); ^{31}P NMR ($CDCl_3$) δ 24.1 (J_{Pt-P} = 1874 Hz). Anal. Calcd for $C_{46}H_{38}P_2Pt$: C, 65.17; H, 4.52. Found: C, 64.31; H, 4.29. Data for **9-^{13}CH$_3$:** ^{31}P NMR ($CDCl_3$) δ 24.3 (J_{Pt-P} = 1755 Hz, J_{C-P} = 96, 17 Hz). ^{13}C NMR ($CDCl_3$) δ 11.7 (J_{Pt-C} = 493 Hz, J_{P-C} = 95, 5 Hz).

Preparation of Pt(CH$_3$)$_2$\{(*R*)-BISPHOSPHITE\} (10 and 10-^{13}CH$_3$). To a solution of (*R*)-BISPHOSPHITE (94.9 mg, 0.13 mmol) in dichloromethane (5 mL) was added Pt(CH$_3$)$_2$(COD) (42.5 mg, 0.13 mmol), and the solution was stirred at room temperature for 2.5 h. The clear solution was concentrated and dried *in vacuo* to give a colorless solid (130.1 mg, 99% yield): ^{1}H NMR ($CDCl_3$) δ 0.41 (J_{Pt-H} = 70.6 Hz), 6.26 (d, J = 8.3 Hz), 6.8−7.9 (m); ^{31}P NMR ($CDCl_3$) δ 125.4 (J_{Pt-P} = 3043 Hz). Anal. Calcd for $C_{46}H_{38}O_6P_2Pt$: C, 58.54; H, 4.06. Found: C, 58.48; H, 4.08. Data for **10-^{13}CH$_3$:** ^{31}P NMR ($CDCl_3$) δ 125.5 (J_{Pt-P} = 3041 Hz, J_{C-P} = 154, 24 Hz); ^{13}C NMR ($CDCl_3$) δ 2.6 (J_{Pt-C} = 574 Hz, J_{P-C} = 153, 24 Hz).

Preparation of Pt(CH$_3$)Cl\{(*R,S*)-BINAPHOS\}. Pt(CH$_3$)Cl(COD) (197.7 mg, 0.56 mmol) and (*R,S*)-BINAPHOS (431.2 mg, 0.56 mmol) were dissolved in dichloromethane (20 mL) by stirring at room temperature for 1.5 h. The resulting clear solution was concentrated and dried *in vacuo.* Recrystallization of the product from CH_2Cl_2/Et_2O gave a colorless solid (415.9 mg, 73% yield): ^{1}H NMR ($CDCl_3$) δ 1.30 (J_{Pt-H} = 60.0 Hz, J_{P-H} = 7.8, 3.4 Hz), 4.66 (d, J = 8.9 Hz), 5.86 (d, J = 8.6 Hz), 6.6−8.2 (m); ^{31}P NMR ($CDCl_3$) δ 23.0 (J_{Pt-P} = 1402 Hz, J_{P-P} = 26 Hz), 115.2 (J_{Pt-P} = 7562 Hz, J_{P-P} = 26 Hz). Anal. Calcd for $C_{53}H_{37}ClO_3P_2Pt$: C, 62.76; H, 3.68. Found: C, 62.47; H, 3.68.

Preparation of Pt(CH$_3$)Cl\{(*R*)-BINAP\}. Pt(CH$_3$)Cl(COD) (45.1 mg, 0.13 mmol) and (*R*)-BINAP (82.1 mg, 0.13 mmol) were dissolved in dichloromethane (1 mL) by stirring at room temperature for 2 h. The reaction mixture was concentrated and dried *in vacuo.* Purification by silica-gel column chromatography (CH_2Cl_2) gave the product (108.8 mg, 96% yield): ^{1}H NMR ($CDCl_3$) δ 0.54 (J_{Pt-H} = 54.8 Hz, J_{P-H} = 7.6, 4.3 Hz), 6.6−7.9 (m); ^{31}P NMR ($CDCl_3$) δ 19.0 (J_{Pt-P} = 4446 Hz, J_{P-P} = 15 Hz), 24.4 (J_{Pt-P} = 1753 Hz, J_{P-P} = 15 Hz). Anal. Calcd for $C_{45}H_{35}ClP_2Pt$: C, 62.25; H, 4.06. Found: C, 62.38; H, 4.31.

Preparation of Pt(CH$_3$)Cl\{(*R*)-BISPHOSPHITE\}. To a solution of (*R*)-BISPHOSPHITE (44.7 mg, 0.062 mmol) in dichloromethane (5 mL) was added Pt(CH$_3$)Cl(COD) (22.2 mg, 0.063 mmol), and the solution was stirred at room temperature for 1 h. The reaction mixture was concentrated and dried *in vacuo.* Purification by silica gel column chromatography (CH_2Cl_2) gave the product (54.9 mg, 92% yield): ^{1}H NMR ($CDCl_3$) δ 0.78 (J_{Pt-H} = 54.8 Hz, J_{P-H} = 10.6, 3.3 Hz), 6.17 (d, J = 8.3 Hz), 6.40 (d, J = 8.2 Hz), 6.7−8.0 (m); ^{31}P NMR ($CDCl_3$) δ 81.0 (J_{Pt-P} = 7047 Hz, J_{P-P} = 37 Hz), 125.0 (J_{Pt-P} = 2682 Hz, J_{P-P} = 37 Hz). Anal. Calcd for $C_{45}H_{35}ClO_6P_2Pt$: C, 56.05; H, 3.66. Found: C, 56.12; H, 3.75.

Preparation of PtCl$_2$\{(*R,S*)-BINAPHOS\}. After a mixture of PtCl$_2$(COD) (28.7 mg, 0.077 mmol) and (*R,S*)-BINAPHOS (60.6 mg, 0.079 mmol) in dichloromethane (2 mL) was stirred at room temperature for 30 min, the resulting clear solution was concentrated and dried *in vacuo* to give a white solid (73.0 mg, 92% yield): ^{1}H NMR ($CDCl_3$) δ 4.54 (d, J = 7.9 Hz), 5.83 (d, J = 8.3 Hz), 6.6−8.6 (m); ^{31}P NMR ($CDCl_3$) δ 8.2 (J_{Pt-P} = 3243 Hz, J_{P-P} = 18 Hz), 103.8 (J_{Pt-P} = 6270 Hz, J_{P-P} = 18 Hz). Anal. Calcd for $C_{52}H_{34}Cl_2O_3P_2Pt$: C, 60.36; H, 3.31. Found: C, 59.79; H, 3.13.

Preparation of PtCl$_2$\{(*R*)-BISPHOSPHITE\}. A mixture of (*R*)-BISPHOSPHITE (110.3 mg, 0.15 mmol) and PtCl$_2$(COD) (56.3 mg, 0.15 mmol) was stirred in dichloromethane (5 mL) at room temperature for 18 h, and then the resulting clear solution was concentrated and dried *in vacuo* to give a colorless solid (147.1 mg, 99% yield): ^{1}H NMR ($CDCl_3$) δ 6.28 (d, J = 7.9 Hz), 6.7−8.0 (m); ^{31}P NMR ($CDCl_3$) δ 61.9 (J_{Pt-P} = 5672 Hz). Anal. Calcd for $C_{44}H_{32}Cl_2O_6P_2Pt$: C, 53.67; H, 3.28. Found: C, 53.51; H, 3.30.

Preparation of Cationic Complex (*SP*-4-3)-[Pt(CH$_3$)(CH$_3$CN)\{(*R,S*)-BINAPHOS\}]·[B\{3,5-(CF$_3$)$_2$C$_6$H$_3$\}$_4$] (11). A mixture of Pt(CH$_3$)Cl((*R,S*)-BINAPHOS) (53.6 mg, 0.053 mmol) and NaB[3,5-(CF$_3$)$_2$C$_6$H$_3$]$_4$ (46.6 mg, 0.053 mmol) was dissolved in dichloromethane (10 mL) and acetonitrile (0.2 mL, 3.8 mmol) and stirred at room temperature for 5 h. The reaction mixture was concentrated and dried *in vacuo* to give **11** as a colorless solid (99.7 mg, 99% yield): ^{1}H NMR ($CDCl_3$) 1.12 (br t, J_{Pt-H} = 61.0 Hz, CH_3Pt), 1.72 (s, CH_3CN); ^{31}P NMR ($CDCl_3$) δ 22.9 (phosphine, J_{Pt-P} = 1476 Hz, J_{P-P} = 29 Hz), 103.5 (phosphite, J_{Pt-P} = 7935 Hz, J_{P-P} = 29 Hz).

Replacement of CH$_3$CN of 11 by CO To Give (*SP*-4-3)-[Pt(CH$_3$)(CO)\{(*R,S*)-BINAPHOS\}]·[B\{3,5-(CF$_3$)$_2$C$_6$H$_3$\}$_4$] (12a). To a mixture of Pt(CH$_3$)Cl\{(*R,S*)-BINAPHOS\} (60.4 mg, 0.0596 mmol) and Na-[B\{3,5-(CF$_3$)$_2$C$_6$H$_3$\}$_4$] (53.9 mg, 0.0608 mmol) was added dichloromethane saturated with CO (5 mL). After being stirred at room temperature for 4 h, the reaction mixture was concentrated and dried *in vacuo* to give a white solid. Data for **12a**: ^{31}P NMR ($CDCl_3$) δ 15.4 (J_{Pt-P} = 1567 Hz, J_{P-P} = 37 Hz), 121.8 (J_{Pt-P} = 6023 Hz, J_{P-P} = 37 Hz); ^{1}H NMR ($CDCl_3$) δ 1.45 (J_{Pt-H} = 55.0 Hz, J_{P-H} = 6.3 Hz), 4.74 (d, J = 8.9 Hz), 5.89 (d, J = 8.6 Hz), 6.6−8.4 (m); IR ($CHCl_3$) 2132 cm^{-1} (ν_{CO}).

Isomerization of Cationic Carbonyl Complex 12a to 12b. A solution of **12a** (37.5 mg) in dichloromethane (10 mL) was placed in an autoclave. Carbon monoxide was introduced (20 atm), and the mixture was stirred at room temperature for 20 h. After the pressure was released, the reaction mixture was transferred to a Schlenk tube and concentrated and dried *in vacuo*. A white solid was obtained. Data for **12b**: ^{31}P NMR ($CDCl_3$) δ 14.9 (J_{Pt-P} = 3265 Hz, J_{P-P} = 40 Hz), 148.3 (J_{Pt-P} = 3029 Hz, J_{P-P} = 40 Hz); ^{1}H NMR ($CDCl_3$) δ 0.53 (J_{Pt-H} = 54.8 Hz, J_{P-H} = 8.2, 6.6 Hz), 4.80 (d J = 8.9 Hz), 5.94 (d J = 8.6 Hz), 6.6−8.4 (m); IR ($CHCl_3$) 2128 cm^{-1} (ν_{CO}). CO insertion to give the corresponding acylplatinum did not proceed.

Observation of the Rapid Equilibrium between 4a and 4b. A 4:1 mixture of **4a** and **4b** in $CDCl_3$ (0.5 mL) and CD_3CN (0.1 mL) was treated with CO (1 atm) at 20 °C, and the reaction was followed by ^{1}H and ^{31}P NMR. After 2 h, 30% of **4** was converted to **5-D**, without changing the isomeric ratio of **4a** and **4b**.

Computational Details for the Process 3 → 14 → 4. The geometries of transition states, **ts(14a′-4a′)** and **ts(14b′-4b′)** as well as reactants **14a′** and **14b′** and products **4a′** and **4b′** were fully optimized using the hybrid density functional method B3LYP with the LANL2DZ basis set, called basis set I in this paper, which includes for the Pd atom an effective core potential replacing core electrons up to 3d and double ζ valence basis functions (8s6p4d)/[3s3p2d] by Hay and Wadt[29] and for the ligand atoms the Huzinaga−Dunning valence double ζ basis functions.[30] In order to obtain more reliable energetics, we carried out energy calculations by the B3LYP method and by the Møller−Plesset perturbation theory at the second (MP2) up to the fourth order without triple substitution (MP4SDQ). In these energy calculations we used better basis set, called basis set II, in which the triple ζ contraction of Pd d orbitals was adopted and the single set of f orbitals with an exponent of 1.472 was augmented.[31] For the ligand atoms were used 6-31G(d,p) basis functions.[32] In the calculation of the zero-point energy and thermal correction to a potential energy, the vibrational frequencies were scaled with a factor of 0.9614.[33] All the ab initio molecular orbital

(29) Hay, P. J.; Wadt, W. R. *J. Chem. Phys.* **1985**, *82*, 299.
(30) Dunning, T. H. *J. Chem. Phys.* **1971**, 55, 716.
(31) Ehlers, A. W.; Böhme, M.; Dapprich, S.; Gobbi, A.; Höllwarth, A.; Jonas, V.; Köhler, K. F.; Stegmann, R.; Veldkamp, A.; Frenking G. *Chem. Phys. Lett.* **1993**, *208*, 111.
(32) (a) Hehre, W. J.; Ditchfield, R.; Pople, J. A. *J. Chem. Phys.* **1972**, *56*, 2257. (b) Hariharan, P. C.; Pople, J. A. *Theor. Chim. Acta* **1973,** *28*, 213.
(33) Scott, A. P.; Radom, L. *J. Phys Chem.* **1996**, *100*, 16502.

and density functional calculations were carried out using the GAUSSIAN94 program.[34]

While **14b′** is more stable than **14a′** at all the levels using basis set II, the B3LYP/I calculation gave the reverse result that **14a′** is more stable than **14b′**. In addition, the Pd−acyl bond in **14a′** is shorter than that in **14b′**, different from the trend in **8** where the Pt−methyl bond *trans* to phosphine is shorter than that *trans* to phosphite. In order to evaluate the reliability of the B3LYP/I method, we calculated the proton affinity of PH_3 and $P(OH)_3$, in which the structures were determined at the B3LYP/I level, and furthermore the energies were calculated at the B3LYP/II level. The calculations showed that at the B3LYP/I level the proton affinity of PH_3 is 19.8 kcal/mol larger than that of $P(OH)_3$, whereas at the B3LYP/II//B3LYP/I level it is smaller by 16.3 kcal/mol. The B3LYP/II geometry determinations did not change the trend. The larger *trans* influence of phosphite seems to correlate with this larger proton affinity of $P(OH)_3$. Use of polarization functions is indispensable to reproduce the difference in electronic effects between phosphine and phosphite. Although the B3LYP/I calculations did not reproduce the difference in bond distances, the calculations of proton affinity clearly demonstrate that the energy calculations with basis set II at the B3LYP/I structures are reliable. Similarly at the B3LYP/I level **4b′** is more stable than **4a′**, and the calculations with basis set II gave the correct results.

The structures of the transition states have several points to be remarked. At **ts(14a′-4a′)**, the newly forming CC bond (1.862 Å) is 0.06 Å shorter than that of **ts(14b′-4b′)** (1.922 Å). The Pd−acyl bond at **ts(14a′-4a′)** (2.336 Å) is stretched by 0.31 Å, whereas that at **ts(14b′-4b′)** is stretched by only 0.23 Å. These results show that **ts(14b′-4b′)** is located earlier, consistent with the larger exothermicity of the reaction of **14b′** to **4b′** at the B3LYP/I level. However, the calculations with basis set II showed that the reaction of **14a′** to **4a′** is more exothermic, and thus **ts(14a′-4a′)** would be located earlier at a higher level of calculations.

Second, one can notice that one of the hydroxy hydrogens of $P(OH)_3$ at **ts(14b′-4b′)** is close to the acyl oxygen, its distance of 2.433 Å suggesting weak hydrogen bonding between them. However, this hydrogen bonding does not exist in a real complex with the BINAPHOS ligand, since BINAPHOS does not have hydroxy groups. In order to assess the stabilization of **ts(14b′-4b′)** by this hydrogen bonding, we determined the structure of **ts(14b′-4b′)**, fixing the H−O−P−Pd dihedral angle to be 178.4° and P(phosphine)−Pd−P−O to be 150.0°, which are those determined by the integrated molecular orbital plus molecular mechanics method[35] for **I**. These restrictions destabilized **ts(14b′-4b′)** by 2.4 kcal/mol at both B3LYP/II and MP4SDQ/II levels. The reactant **14b′** is also destabilized by the same restrictions by 0.9 and 0.7 kcal/mol at the B3LYP and MP4SDQ/II levels, respectively, and consequently the hydrogen bonding decreases the activation energy for path B by only 1.5−1.7 kcal/mol. Without hydrogen bonding the activation energy for path B is slightly larger than that for path A. However, such a small effect would be negligible compared with errors due to modeling or approximation in computational methods. At the present level of calculations it is safer to say that path B passing through **4b′** and **ts(14b′-4b′)** is more favorable because of the larger stability of **4b′** compared with **4a′**. Note that **ts(14b′-4b′)** is always more stable than **ts(14a′-4a′)**.

In molecular mechanics (MM) calculations, PH_3 and $P(OH)_3$ were replaced by (*R*,*S*)-BINAPHOS, and one of the hydrogen atoms of ethene was replaced by a methyl group. The Cartesian coordinates of the propene methyl group and all the atoms but phosphorous atoms of the BINAPHOS ligand were optimized, whereas the B3LYP optimized geometries, excluding the replaced hydrogen atoms of PH_3 and ethene and hydroxyl groups of $P(OH)_3$, were frozen, which is called the combined MO + MM method.[36] We used the MM3 program in the calculations.[37] The standard MM3 parameters are used when available. The van der Waals parameters reported by Rappé *et al.* are used for the Pd atom.[38]

Kinetic Experiments. (1) Propene Insertion into 3 To Give 4. The acylpalladium **3** (12.0 mg, 6.8 μmol) was dissolved in $CDCl_3$ (0.6 mL) under Ar in an NMR tube. The solution was degassed by the freeze−thaw method and then saturated with 1 atm of propene at −78 °C. When the solution became homogeneous, the mixture was warmed to −10 °C. The appearance of the doublet due to the methyl protons of **4**, originating from propene, was monitored in relation to the unchanging aromatic protons to determine the first-order rate constant for the reaction. Spectra were recorded every 15 min in the first 1 h and after that every hour for 4 h at −10 °C. The rate constant ($k_{obs} = (5.3 \pm 2.0) \times 10^{-4}$, $\Delta G^{\ddagger} = 19.3 \pm 0.2$ kcal/mol) was determined from the slope of the line from ln [4-CH_3/aromatic H] versus time. The same experiment was repeated five times to estimate the error. The rate was measured at 0 °C in the same manner ($k_{obs} = 11.8 \times 10^{-4}$, $\Delta G^{\ddagger} = 19.6$ kcal/mol, $R^2 = 0.931$). Both experiments were duplicated.

(2) CO Insertion into 4 To Afford 5. The alkylpalladium **4** (15.0 mg, 8.2 μmol) was dissolved in $CDCl_3$ (0.6 mL) under Ar in an NMR tube. One equivalent of CH_3CN (0.40 μL, 7.7 μmol) was added, and then the solution was saturated by CO under 1 atm by the freeze−thaw method. After the solids were dissolved at −78 °C, the NMR tube was put into a cooled autoclave at −10.0 °C. Under a CO pressure of 20 atm, the reaction was checked after 71, 151, and 319 min by release−repressurize of CO to measure ^{1}H NMR under 1 atm of CO at −23 °C. The reaction did not proceed under 1 atm of CO at this temperature, and thus the time for recording the spectra was omitted from the reaction time. The decay of the CH_3 signal of **4** relative to the unchanging aromatic protons was used to determine the first-order rate constant for the reaction. The rate constant ($k_{obs} = 1.20 \times 10^{-4}$, $\Delta G^{\ddagger} = 19.0$ kcal/mol, $R^2 = 0.993$) was determined from the slope of the line from −ln [4-CH_3/aromatic H] versus time. The rate was measured at −12 °C in the same manner ($k_{obs} = 1.16 \times 10^{-4}$, $\Delta G^{\ddagger} =$ 18.9 kcal/mol, $R^2 = 0.991$).

Asymmetric Copolymerization of Propene with CO Catalyzed by [Pd(CH$_3$)(CH$_3$CN){(*R*,*S*)-BINAPHOS}]·[B{3,5-(CF$_3$)$_2$C$_6$H$_3$}$_4$] (2). A solution of (*R*,*S*)-BINAPHOS (8.7 mg, 0.011 mmol) in benzene (0.5 mL) was added to a solution of Pd(CH_3)(Cl)(COD) (3.0 mg, 0.011 mmol) in benzene (1.0 mL). The solution was stirred at 20 °C for 1 h and concentrated *in vacuo*. The product was dissolved with CH_2Cl_2 (1.0 mL), and then to the solution was added a solution of NaB(3,5-$(CF_3)_2C_6H_3)_4$ (10.0 mg, 0.011 mmol) in CH_3CN (1.0 mL). After the solution was stirred at 20 °C for 1 h, the solvents were removed. The residue was dissolved in CH_2Cl_2 (2 mL) and was degassed by three cycles of freeze−thaw. After being treated with CO (1 atm), the solution was charged with propene (3 atm, 50 mL). The mixture was stirred under CO (20 atm) for 4 days at 20 °C. After the pressure was released, 0.2 mL of CH_3OH was added, and the mixture repressurized with CO in order to cleave the Pd−C bond by carbomethoxylation. After 1 h, the reaction mixture was poured into CH_3OH (100 mL) under air to precipitate poly(propene-*alt*-CO) (0.333 g, 76% yield): T_m = 164 °C; T_g = 8 °C; M_w = 104 400; M_n = 65 300; M_w/M_n = 1.6; ^{1}H NMR ((CF$_3$)$_2$CDOD) δ 1.03 (d, J = 6.93 Hz, 3H, CH_3), 2.52 (dd, J = 16.83, 1.98 Hz, 1H, C*H*H), 2.88−3.09 (m, 2H, CH*H* and C*H*CH$_3$); ^{13}C NMR ((CF$_3$)$_2$CDOD) δ 15.8, 41.5, 44.9, 218.0; IR (Nujol) 1705 (CO) cm^{-1}; $[\phi]^{24}_D = +40°$ (*c* 0.51, (CF$_3$)$_2$CHOH).

Asymmetric Copolymerization of (4-*tert*-Butylphenyl)ethene with CO Catalyzed by [Pd(CH$_3$)(CH$_3$CN){(*R*,*S*)-BINAPHOS}]·[B{3,5-(CF$_3$)$_2$-C$_6$H$_3$}$_4$] (2). A solution of **2** (0.011 mmol) in CH_2Cl_2 (1.0 mL) was degassed by three cycles of freeze−thaw. After the solution was treated with CO (1 atm), (4-*tert*-butylphenyl)ethene (1.77 g, 11.0 mmol) was added. The mixture was stirred under CO (20 atm) for 4 days at

(34) Gaussian 94: M. J. Frisch, G. W. Trucks, H. B. Schlegel, P. M. W. Gill, B. G. Johnson, M. A. Robb, J. R. Cheeseman, T. Keith, G. A. Petersson, J. A. Montgomery, K. Raghavachari, M. A. Al-Laham, V. G. Zakrzewski, J. V. Ortiz, J. B. Foresman, J. Cioslowski, B. B. Stefanov, A. Nanayakkara, M. Challacombe, C. Y. Peng, P. Y. Ayala, W. Chen, M. W. Wong, J. L. Andres, E. S. Replogle, R. Gomperts, R. L. Martin, D. J. Fox, J. S. Binkley, D. J. Defrees, J. Baker, J. P. Stewart, M. Head-Gordon, C. Gonzalez, and J. A. Pople, Gaussian, Inc., Pittsburgh, PA, 1995.

(35) (a) Maseras, F. Morokuma, K. *J. Comput. Chem.* **1995**, *16*, 1170. (b) Matsubara, T.; Sieber, S. Morokuma, K. *Int. J. Quantum Chem.* **1996**, *60*, 1101. (c) Matsubara, T.; Maseras, F.; Koga, N.; Morokuma, K. *J. Phys. Chem.* **1996**, *100*, 2573.

(36) (a) Kawamura-Kuribayashi, H.; Koga, N.; Morokuma, K. *J. Am. Chem. Soc.* **1992**, *114*, 8687. (b) Maseras, F.; Koga, N.; Morokuma, K. *Organometallics* **1994**, *13*, 4008. (c) Yoshida, T.; Koga, N.; Morokuma, K. *Organometallics* **1996**, *15*, 766.

(37) Allinger, N. L. *mm3(92)*; QCPE: Bloomington, IN, 1992.

(38) Rappé, A. K.; Casewit, C. J.; Colwell, K. S. Goddard, W. A., III; Skiff, W. M. *J. Am. Chem. Soc.* **1992**, 114, 10024.

20 °C and then treated with CH_3OH (100 mL) to precipitate poly((4-*tert*-butylphenyl)ethene-*alt*-CO) (0.224 g, 11% yield): T_m = 158 °C; T_g = 122 °C; M_w = 5600; M_n = 4300; M_w/M_n = 1.3; ^{1}H NMR ($CDCl_3$) δ 1.24 (s, 9H, $C(CH_3)_3$), 2.59−2.74 (m, 1H, C*H*H), 3.10−3.20 (m, 1H, CH*H*), 3.89−4.10 (m, 1H, CH), 6.85 (d, J = 8.25 Hz, 2H, Ar), 7.12 (d, J = 8.25 Hz, 2H, Ar); ^{13}C NMR ($CDCl_3$) δ 31.3, 34.4, 45.6, 51.7, 125.6, 127.8, 134.4, 149.9, 207.0; IR (Nujol) 1711 (CO) cm^{-1}; $[\phi]^{23}_D$ −492° (*c* 0.50, CH_2Cl_2).

Attempted CO and Propene Insertion into [Pd(COCH$_3$)(CH$_3$CN)-{(*R*)-BINAP}]·[B{3,5-(CF$_3$)$_2$C$_6$H$_3$}$_4$]. A solution of [Pd(CH_3)(CH_3-CN){(*R*)-BINAP}]·[B{3,5-$(CF_3)_2C_6H_3$}$_4$] (6.0 mg, 6.5 × 10^{-3} mmol) in $CDCl_3$ (0.5 mL) was treated with CO (1 atm) at room temperature for 1 h to give [Pd($COCH_3$)(S){(*R*)-BINAP}]·[B{3,5-$(CF_3)_2C_6H_3$}$_4$]. Three species have been characterized by ^{31}P NMR (the ratio was about 1:1:1). From ^{1}H NMR, two of them were assigned to be acyl complexes: ^{1}H NMR ($CDCl_3$) δ 2.37 (CH_3CN), 2.17 (d, J = 2.0 Hz, C*H*$_3$COPd), 2.04 (d, J = 7.9 Hz, C*H*$_3$COPd); ^{31}P NMR ($CDCl_3$) δ 21.3 (d, J_{P-P} = 55 Hz), 23.7 (d, J_{P-P} = 55 Hz); 20.6 (d, J_{P-P} = 54 Hz), 23.9 (d, J_{P-P} = 54 Hz); 12.6 (d, J_{P-P} = 66 Hz), 24.9 (d, J_{P-P} = 66 Hz). A solution of the above mixture (6.0 mg, 0.0065 mmol) in $CDCl_3$ (0.5 mL) was treated with propene (1 atm) at room temperature for 20 h. A new pair of peaks were observed by ^{31}P NMR, but the conversion was lower than 10%: ^{31}P NMR ($CDCl_3$) δ 38.0 (d, J_{P-P} = 44 Hz), δ 16.0 (d, J_{P-P} = 44 Hz).

***(E)*-2-Butene Insertion into 3.** The acylpalladium complex **3** (6.0 mg, 0.0065 mmol) was prepared as described above and dissolved in $CDCl_3$ (0.5 mL). The solution was degassed by three freeze−thaw cycles and treated with *(E)*-2-butene (1 atm) for 14 h to give the corresponding alkylpalladium complexes **16a** and **16b** as an almost 1:1 mixture. Data for **16a**: ^{31}P NMR ($CDCl_3$) δ 143.0 (d, J_{P-P} = 64 Hz), 13.0 (d, J_{P-P} = 64 Hz). Data for **16b**: δ 141.1 (d, J_{P-P} = 67 Hz), 13.6 (d, J_{P-P} = 67 Hz). *(Z)*-2-Butene was treated similarly to give the identical ^{31}P NMR chart.

Acknowledgment. K.N. thanks Professor M. A. Bennett (Australian National University) for helpful discussions. K.N. and N.K. are grateful for Grants-in-Aid for Scientific Research on Priority Area "New Polymers and Their Nano-Organized Systems" (No. 08246231) and for Scientific Research (C) (No. 09650901), respectively, from the Ministry of Education, Science, Sports, and Culture, Japan. Part of the calculations were carried out at the Computer Center of the Institute for Molecular Science, Japan.

Supporting Information Available: X-ray data of [Pd{CH_2-$CH(CH_3)CO$}{(*R*,*S*)-BINAPHOS}]·[B{3,5-$(CF_3)_2C_6H_3$}$_4$] and Pt(CH_3)$_2${(*R*,*S*)-BINAPHOS} (29 pages). See any current masthead page for ordering and Internet access instructions.

JA973199X